



UPPSALA  
UNIVERSITET

# Investigation of unknown groundwater flows to two leachate ponds at Hovgården

Undersökning av okända grundvattenflöden till lakdammar på  
Hovgården

---

Katja Nordström

## Abstract

*Katja Nordström*

The leaching of groundwater into two polishing ponds, the last step in the wastewater treatment process on Hovgården waste facility, was examined. The focus of this study was to analyse the PFAS composition profile (fingerprint) to trace the leaching groundwater. PFASs are very persistent man-made substances, used in various fields and have been linked to several health issues. Polishing pond data and groundwater data for ions and PFAS was collected, compiled with old data and surveyed, mainly by using principle component analysis (PCA). The results indicate that there is a water flow and a mass flow of ions to the ponds, and possibly also a flow of PFAS. The ponds appear to have a different composition, which possible could be the result of a mass flow, however the macro ion distribution is similar. Of the groundwater wells, data suggests that 18G09, P3 IN and P8 were most affected by the landfill. PFOA was the most detected PFAS, and the sampling points with the highest concentration of PFAS was 18G09, P3 IN and the first sampling point (R1) in the wastewater treatment plant. While no apparent correlation between the polishing ponds and groundwater wells were discovered, data suggest that the leaching may come from some of the wells more affected by the landfill.

**Keywords:** landfill, leachate, principle component analysis, PCA, polishing pond.

*Department of Earth Sciences, Uppsala University, Villavägen 16, SE-752 36 Uppsala, Sweden. ISSN 1401–5765.*

# Referat

*Katja Nordström*

På Hovgården, en deponi strax utanför Uppsala, har det noterats att vatten läcker in i de två polerdammarna på området, som utgör det sista steget i reningen av lakvattnet. Syftet med den här studien var att undersöka det här okända flödet och dess effekter på polerdammarna, samt att försöka spåra det till någon av grundvattenbrunnarna på området. Fokus lades på att undersöka PFAS-sammansättningen (fingerprint) i flödet med principalkomponentanalys (PCA). PFAS är persistenta ämnen som har används inom en mängd områden. De är ett resultat av mänsklig aktivitet och är kopplade till flera hälsorisker. Data från polerdammarna samt grundvattendata insamlades och sammanställdes med gamla data, främst genom PCA. Data indikerar att det finns ett flöde av vatten och ämnen, och möjligtvis också PFAS, till dammarna. Data pekar också på att de båda dammarna har olika sammansättning, även om makrojonssammansättningen är lika, vilket skulle kunna bero på massflödet. De grundvattenbrunnar på Hovgården som pekades ut som mest påverkade av deponin var 18G09, P3 IN and P8. PFOA var den PFAS som detekterades i flest provpunkter och de punkter med högst PFAS-koncentration var 18G09, P3 IN och den första provtagningspunkten i reningsverket (R1). Ingen tydlig koppling mellan någon grundvattenbrunn och polerdammarna kunde påvisas, men resultaten indikerar att inläckaget härstammar från det mer påverkade grundvattnet.

**Nyckelord:** deponi, lakvatten, principalkomponentanalys, PCA, polerdammar.

## Preface

This master thesis completes my studies at the Master's Programme in Environmental and Water Engineering, and it would not exist without the help of my supervisor and subject reviewer; thank you Sofia Seroka Bjälkefur, Uppsala Vatten och Avfall AB, for your good advices, support, enthusiasm and all the help you provided during the sampling! Also, big thanks for your very informative map of the groundwater wells at Hovgården I could include in this thesis. Thank you Lutz Ahrens, Department of Aquatic sciences, Swedish University of Agriculture, for generously sharing your knowledge, your support and for patiently answering all my questions.

Thank you Uppsala Vatten och Avfall AB for letting me use two of your wonderful pictures of Hovgården.

Thank you Dan Berggren Kleija for answering my questions regarding ion interaction in soil and water. It was most helpful!

Lastly, I want to thank my family and all of my friends. You have been so important during these years and I am very grateful. This work would not have been possible without your endless support.

*Copyright © Katja Nordström and Department of Aquatic Sciences and Assessment, SLU.*

*UPTEC W 23016, ISSN 1401–5765.*

*Digitally published in DiVA, 2023, through the Department of Earth Sciences, Uppsala University. (<http://www.diva-portal.org/>)*

## Populärvetenskaplig sammanfattning

Vi människor producerar mängder av avfall som, om det inte kan återvinnas, hamnar på deponier. Men farliga ämnen i avfallet försvinner inte, utan de kan läcka ut i naturen igen om man inte tar hand om avfallet på ett ordentligt sätt. Ett sådant ämne är PFAS, som de senare åren har blivit alltmer omtalat på grund av dess stabilitet och den risk som PFAS kan utgöra mot människors hälsa. Att veta hur vatten rör sig på en deponi är därför viktigt för att skydda omgivningen.

Deponin Hovgården ligger ca 12 kilometer utanför Uppsala, Sverige. Den har varit i drift sedan början av 70-talet och än idag är delar av deponin aktiv och tar emot icke-farligt avfall. Området fyller idag flera funktioner: här sorteras återvunna fraktioner, slam från Uppsalas reningsverk mellanlagras och som återvinningsstation för allmänheten. När vattnet rinner igenom avfallet deponin bildas lakvatten, som samlas upp på de hårdgjorda ytorna på deponin. Lakvatten från deponier är ofta mycket förorenat och måste renas innan det släpps ut, för att det inte ska ha skadliga effekter på människa och natur. På Hovgården finns sedan 2007 det nuvarande reningsverket, som renar lakvattnet i flera steg. I det näst sista steget, innan vattnet luftas och släpps ut i recipienten Hovgårdsbäcken, hamnar vattnet i två polerdammar. Vid det här laget har majoriteten av lakvattenreningen skett, men här tillåts partiklar som kan finnas kvar i vattnet att sjunka till botten i lugn och ro. Sedan är vattnet tillräckligt rent för att släppas tillbaka i naturen igen, ut i Hovgårdsbäcken.

Hovgårdens deponi är välövervakad och man provtar regelbundet både ytvatten och grundvatten på området. Det var så de anställda på Hovgården lade märke till att något märkligt skedde i polerdammarna. De misstänkte att ett okänt flöde rann till och påverkade vattenkvaliteten. Man märkte också att det rann ut mer vatten än vad som rann in. Det blev ett detektivarbete att försöka svara på frågorna: varifrån kommer vattnet, och var läcker det in?

Det första steget i att lösa den här gåtan var att bevisa misstanken om att det faktiskt fanns ett tillflöde till polerdammarna. Genom att titta på koncentrationer och flöden in och ut ur dammarna kunde man dra slutsatsen att det verkligen tillkom vatten från en okänd källa. Det gick också att uppskatta koncentrationen i det här okända flödet. Det var dock svårt att säga om det bara var ett flöde, eller om det fanns flera. I så fall var den beräknade koncentrationen en medelkoncentration i de okända flödena.

Som tidigare nämnt så är det svårnedbrytbara ämnet PFAS vanligt på en deponi, vilket kunde utnyttjas i ett försök att lösa gåtan om det okända flödet. PFAS är nämligen inte ett ämne, utan ett samlingsnamn för flera ämnen med liknande utseende och egenskaper. Genom att analysera proportionerna mellan de olika

PFAS-ämnena kunde ett slags fingeravtryck skapas för varje provpunkt. Punkter som är lika varandra, till exempel att samma typ av avfall lagras där, borde också ha liknande PFAS-sammansättning. Om PFAS från en viss plats på deponin hamnar i grundvatten som senare läcker in i det rena vattnet i polerdammarna, är det i teorin inte omöjligt att spåra från vilken grundvattenbrunn det inläckande vattnet härstammar från genom att jämföra fingeravtryck.

Om man har mycket data kan det vara svårt att se samband. Då kan det vara bra att använda statistiska verktyg som minskar mängden data, men bevarar viktiga samband. I den här studien användes principalkomponentanalys, PCA, som är ett sådant verktyg. När man presenterar data i en PCA-figur är det mycket lättare att se samband.

Så lyckades man spåra vattnet från polerdammarna tillbaka till sin källa? Svaret är: nej. PCA-analysen som gjordes gav inga raka svar, men tillsammans med data kunde man ringa in grundvattenbrunnar som verkade vara extra förorenade och punkter i den norra polerdammen som betedde sig märkligt. Grundvatten som man visste var mer förorenat hade ett förhållande mellan olika PFAS som liknade det i den norra polerdammen, vilket skulle kunna peka på att det är där vatten läcker in. Men för att kunna dra säkrare slutsatser skulle man behöva mer data och kanske också komplettera med en annan metod.

# Contents

<b>1</b>	<b>Introduction</b>	<b>1</b>
1.1	Purpose . . . . .	1
1.2	Research Limitations . . . . .	2
<b>2</b>	<b>Background</b>	<b>3</b>
2.1	Landfill leachate . . . . .	3
2.2	Mobility of ion in soils . . . . .	4
2.3	Effects caused by seasonality and age of landfill . . . . .	4
2.4	PFASs . . . . .	5
2.4.1	Definition . . . . .	5
2.4.2	Production and Use . . . . .	5
2.4.3	PFAS in Landfills . . . . .	6
2.4.4	PFAS Regulations . . . . .	7
2.5	Statistics . . . . .	8
2.5.1	Principal Component Analysis . . . . .	9
2.5.2	Interpreting PCA plots . . . . .	10
2.5.3	Addressing Missing Values . . . . .	11
<b>3</b>	<b>Method and Material</b>	<b>12</b>
3.1	Hovgården waste facility . . . . .	12
3.1.1	Site description . . . . .	12
3.1.2	Hovgården wastewater treatment . . . . .	13
3.1.3	The polishing ponds . . . . .	14
3.2	Hydrogeological Survey . . . . .	15
3.3	Sampling and Field Measurement . . . . .	17
3.3.1	Groundwater wells . . . . .	17
3.3.2	The polishing ponds . . . . .	18
3.4	Sample analysis . . . . .	23
3.5	Data Treatment . . . . .	24
3.6	Flow and Mass Balance . . . . .	24
3.7	Charge Balance . . . . .	25
3.8	PFAS Fingerprinting . . . . .	25
3.9	PCA for ions and other statistical parameters . . . . .	26
<b>4</b>	<b>Results</b>	<b>27</b>
4.1	Polishing Ponds Analyses . . . . .	27
4.1.1	Polishing pond water quality . . . . .	27
4.1.2	Water and Mass Flow . . . . .	27
4.1.3	Macro ion distribution . . . . .	32

4.1.4	Charge Balance . . . . .	37
4.1.5	PCA for polishing pond data . . . . .	37
4.2	Groundwater Analyses . . . . .	40
4.2.1	Groundwater quality . . . . .	40
4.2.2	PCA for groundwater data . . . . .	42
4.3	PFAS Analyses . . . . .	45
4.3.1	Groundwater . . . . .	45
4.3.2	Ponds and WWTP water . . . . .	50
4.3.3	Correlation analysis . . . . .	54
4.3.4	PCA for PFAS in surface water and groundwater samples . . . . .	55
<b>5</b>	<b>Discussion</b>	<b>57</b>
5.1	Transport of ions and PFASs to the ponds . . . . .	57
5.2	Correlation between surface water and groundwater . . . . .	60
<b>6</b>	<b>Conclusion</b>	<b>61</b>
<b>A</b>	<b>Mass Balance</b>	<b>68</b>
A.1	Sludge Pumping . . . . .	68
<b>B</b>	<b>Charge Balance</b>	<b>68</b>
<b>C</b>	<b>Mass Balance</b>	<b>69</b>
<b>D</b>	<b>PFAS</b>	<b>70</b>
D.1	PFAS abbreviations . . . . .	70
D.2	PFAS concentration - all samples . . . . .	71
D.3	PFAS composition - all samples . . . . .	72
<b>E</b>	<b>Correlation analysis for ions</b>	<b>72</b>
E.1	Correlation table for ions in the polishing ponds . . . . .	72
E.2	Correlation table for ions in groundwater . . . . .	74

## List of Figures

1	An example of a principle component in a 3-dimensional space. The (feigned) data set has been approximated with one PC. After Wold et al. (1987). . . . .	10
2	Hovgården waste facility. Photo by Uppsala Vatten och Avfall <b>2020-06-01</b> . . . . .	13
3	Wastewater flow in the WWTP in Hovgården. MBBR = moving bed biofilm reactor; Sampling points R1-R3 (WWTP), SP (sedimentation pond), and Polishing ponds (PN and PS). . . . .	14
4	The polishing ponds. PN is situated to the right in the figure and PS to the left. Photo by Uppsala Vatten och Avfall <b>2020-06-01</b> . . .	15
5	Map over Hovgården groundwater wells. Figure by Sofia Seroka Bjälkefur. Used with permission. . . . .	17
6	Sampling of groundwater wells in February. Photo by the author (2022-02-09). . . . .	18
7	Sampling points in the polishing ponds. The figure is not according to scale. This is a schematic figure and not the actual shape of the ponds. . . . .	19
8	Sampling of the polishing ponds. Photo by the author <b>2022-05-02</b> . . . . .	20
9	The mean inflow to the ponds and outflow from sampling point A1. The daily data is from 1st of March 2021 to 31st of January 2022. . . . .	28
10	Monthly mass flow of PFAS. Data is from March, June, September and December 2021 for the inflow and from April, June, August, October and December 2021 for the outflow. . . . .	30
11	Macro ion distribution in the polishing ponds in February 23rd, 2022. . . . .	32
12	Macro ion distribution in the sedimentation pond in March 1st, 2022. . . . .	33
13	Mean concentration for macro ions in the polishing ponds (2021-2022) with standard error bars. Note the different unit for manganese, iron and phosphorus. . . . .	34
14	Mean concentration for some metals in the polishing ponds (2021-2022) with standard error bars. . . . .	35
15	Mean concentration for some metals in the polishing ponds (2021-2022) with standard error bars. . . . .	36
16	Mean concentration for some field parameters in the polishing ponds (2021-2022) with standard error bars. . . . .	37
17	PCA using nutrients and heavy metal data from 2021 and 2022 for the polishing ponds using log data. . . . .	39

18	Biplot using nutrients and heavy metal data from 2021 and 2022 for the polishing ponds using log data. . . . .	40
19	Mean of selected groundwater data parameters from 2021 and 2022 with standard error. For bars without standard error, only one sample was available. For 18G14, only one sample for all variables was available. . . . .	42
20	PCA using nutrients and heavy metal data from 2021 and 2022 for groundwater water using log data. . . . .	43
21	Biplot using nutrients and heavy metal data from 2021 and 2022 for groundwater using log data. . . . .	44
22	The fraction of PFAS detected in surface water and groundwater samples. Several other PFASs were included in the analysis, but since they were not detected, they are not included in the plot. . .	45
23	Sum PFAS concentrations in groundwater samples at Hovgården. Values under the detection limit were set to zero. . . . .	46
24	Fractional distribution of PFAS in groundwater in Hovgården. Values under the detection limit were set to zero. . . . .	47
25	Results from the PCA analysis of PFAS composition (fingerprint) in groundwater. November ("nov") samples were sampled in 2021 and March and June ("mar" and "jun", respectively) were sampled in 2022. . . . .	48
26	Results from the PCA analysis of PFAS fingerprint in groundwater. Three samples from 18G02 was excluded in this analysis. November ("nov") samples were sampled in 2021 and March and June ("mar" and "jun", respectively) were sampled in 2022. . . . .	49
27	Results from the PCA analysis of the PFAS composition (fingerprint) in groundwater. Three samples from 18G02 was excluded in this analysis. November ("nov") samples were sampled in 2021 and March and June ("mar" and "jun", respectively) were sampled in 2022. . . . .	50
28	Concentration of PFAS in the WWTP and surface water in Hovgården. Samples under the detection limit was set to zero. . . . .	51
29	PFAS composition profile in the WWTP and surface water in Hovgården. Samples under the detection limit were set to zero. . .	52
30	Results from the PCA analysis of the PFAS composition (fingerprint) in surface water. All sampling points were sampled in March 2022 (Table 1). Sedpond is the sedimentation pond. . . . .	53
31	Biplot of the PCA analysis of the PFAS composition (fingerprint) in surface water. All sampling points were sampled in March 2022 (Table 1). Sedpond is the sedimentation pond. . . . .	54

32	PCA of PFAS composition (fingerprint) for groundwater (red dots) and surface water (blue dots) at Hovgården. The well 18G02 was excluded from the analysis. . . . .	56
33	Biplot of PFAS composition (fingerprint) for groundwater (red dots) and surface water (blue dots) at Hovgården. The well 18G02 was excluded from the analysis. Utlopp seddamm is the sedimentation pond sample, taken by the outlet. . . . .	57
34	Macro ion distribution in the polishing ponds in May 10th, 2022. .	69
35	Concentration of PFAS in Hovgården. For P3 IN, P3 UT and 18G02, samples were taken both in March 2022 and November 2021. . . . .	71
36	PFAS composition profile (fingerprint) of PFAS in Hovgården. For P3 IN, P3 UT and 18G02, samples were taken both in March 2022 and November 2021. . . . .	72
37	Pearson correlation analysis of polishing pond ion data. . . . .	73
38	Pearson correlation analysis of groundwater ion data. . . . .	75

# 1 Introduction

Per- and polyfluoroalkyl substances (PFASs) are substances of increasing concern. PFAS has been linked to several health issues, including reproductive issues, effects on the immune system and cholesterol levels, hormonal effects and lower birth weight (Naturvårdsverket n.d. USEPA 2022). Several PFASs have long degradation time and can be accumulated in the environment and in biota (USEPA 2022). Many PFASs can be transported long distances, because of their high mobility in water, while more volatile PFASs can be transported in air, thus resulting in a widespread distribution (Naturvårdsverket n.d.) all over the globe (KEMI 2022).

Hovgården waste facility is situated approximately 12 kilometers (km) northeast of Uppsala, Sweden. The facility has been used as a landfill since 1971, and parts are still an active landfill for non-hazardous waste. Leachate water from the facility is collected and treated in the on site waste water treatment plant (WWTP). The final step in the waste water treatment process, before the water is aired and released to the recipient, is sedimentation in the polishing ponds. Data from the polishing ponds shows that they are being contaminated by an unknown source, possibly groundwater from the facility. Leachate from landfills poses a risk to human health and to the environment. It is therefore of interest to, if possible, trace where the contamination emanates from and where in the ponds the leaching occurs.

PFAS contamination is common in landfills (Miljösamverkan Sverige 2022) and in Hovgården, significant amounts of PFAS has been measured in different places on the site (Bonnet 2018). There is a need to map out the groundwater flows to possibly trace the source of contamination to the ponds and to prioritize PFAS treatment of groundwater, to ensure safe levels for the recipient. The EU project Life SOuRCE aims to investigate PFAS treatment by a combination of different techniques on two sites in Europe, where one is Hovgården. The results from this master thesis can hopefully give some indication of where on the site PFAS groundwater treatment should be prioritized.

## 1.1 Purpose

The purpose of this master thesis is to survey the water chemistry including ions, metals and PFAS in Hovgården in Uppsala and to investigate how the different groundwater flows contribute to the water quality of the polishing ponds. In addition, the aim is to produce a conceptual model over potential groundwater flows and to calculate their different contributions to the overall water chemistry in the polishing ponds, to improve the treatment process at the landfill in the fu-

ture.

To achieve these goals, five questions were addressed:

- Is there an external water flow entering the polishing ponds?
- Can any conclusions be drawn regarding the composition of this flow?
- Is it possible to use PFAS fingerprinting to trace the water source?
- What effect has the contaminating water on the water quality in the ponds?
- Is there a correlation between surface water (i.e the ponds) and groundwater at Hovgården?

## **1.2 Research Limitations**

To perform this study, old data as well as new data were analysed, however there was a limitation in data. Groundwater is sampled regularly as a part of the annual sampling program through the years, but the polishing ponds had only been sampled a few times during the project time of this master thesis. Therefore, groundwater data was only used during the time period when data from the ponds was available (2021-2022), since the goal was to find a correlation between the water chemistry in groundwater and ponds.

There might also be seasonal variations, such as precipitation and snow melt, but these variations could not be evaluated due to limited data available.

## 2 Background

### 2.1 Landfill leachate

Landfill leachate contains different salts, nutrients, metals and organic substances, which are dissolved by percolating rainwater and surface runoff (Cerne et al. 2007). Different kinds of leachates can be produced on the same landfill: water which percolates through the landfill can differ from water collected from sorting areas, compost areas, etc. (ibid.). Kjeldsen et al. (2002) divide pollutants in leachate into four different groups: organic matter and other organic compounds, inorganic macrocomponents ( $\text{Ca}^{2+}$ ,  $\text{Mg}^{2+}$ ,  $\text{Na}^+$ ,  $\text{K}^+$ ,  $\text{NH}_4^+$ ,  $\text{Fe}^{2+}$ ,  $\text{Mn}^{2+}$ ,  $\text{Cl}^-$ ,  $\text{SO}_4^{2-}$  and  $\text{HCO}_3^-$ ), heavy metals ( $\text{Cd}^{2+}$ ,  $\text{Cr}^{3+}$ ,  $\text{Cu}^{2+}$ ,  $\text{Pb}^{2+}$ ,  $\text{Ni}^{2+}$  and  $\text{Zn}^{2+}$ ) and xenobiotic organic compounds. In addition to these, Kjeldsen et al. (ibid.) mention other elements that can be found in very low concentrations. Östman and Junestedt (2008) have found a number of different compounds in leachate, including different types of mono- and polyaromatic compounds, phenols and cresoles, phthalic esters, chlorinated benzenes and phenols, brominated flame-retardants, pesticides, organic tin and methyl mercury. The researchers also found 49 different metals and elements.

A landfill will go through several phases, which will affect the leachate constitution (Kjeldsen et al. 2002). In the initial phase, when the waste arrives to the landfill, the microbial activity is low but will increase at the end of this phase. Next, in the oxygen- and nitrogen-consuming phase, oxygen and then nitrate are consumed (Östman 2008). As the degradation progresses, oxygen concentrations decrease and the degradation will enter the acidogenic phase, where different acids, hydrogen gas and carbon dioxide are produced. This will result in an increase in conductivity and a large decrease in pH. This phase will then transition into the methanogenic phase, where methane and carbon dioxide are formed. The conductivity decreases and pH increases (Cerne et al. 2007). This is due to the consumption of organic acids and the buffering capacity of the carbonate system (Östman 2008). Metal sulphides will form, resulting in a decrease in the dissolved metal concentration (ibid.) and in sulphate (Kjeldsen et al. 2002). Last is the humus-forming phase, where recalcitrant organic material is left. In this phase, the landfill becomes aerobic (ibid.) and complex organic matter is formed (Östman 2008).

During the different phases, different electron acceptors will be used in degradation. In the oxygen- and nitrogen-consuming phase, oxygen is first used and then nitrogen in the denitrification process. In the anaerobic acidogenic phase, sulphate is reduced and fatty acids are produced through fermentation (Östman 2008; Cerne et al. 2007). In an active landfill, all phases will be present simultaneously

(Cerne et al. 2007). The access to oxygen is crucial for regulating these processes but will also increase the solubility of metals (ibid.). Lower pH will also result in higher solubility of metals (Cimbritz and Jönsson 2017), which is also true for landfill leachate (Abunama et al. 2021). Also the particle content is important, since many contaminants are often bound to particles (Cimbritz and Jönsson 2017).

## **2.2 Mobility of ion in soils**

The availability and mobility of ions in soils depend on the surface interactions with soil particles and soil organic matter. Sorption of substances in soils are govern by ion exchange, adsorption and precipitation (Strawn 2021). How well a compound sorps does not only depend on soil properties but also on the properties of the chemical, such as ion radius, electron configuration of the outer shell and bond properties. Some heavy metals, for example, will absorb by inner-sphere complexation while earth metals will adsorb as outer-sphere complexes (ibid.). A soil property governing the sorption is pH. Surface charge of soil particles and solid organic material with acidic and base functional groups is variable and can change with pH, while some soils with paramount of clay mineral have a permanent charge, unaffected by pH (ibid.). The organic matter content is also important, since it has a large specific surface where chemicals can adsorb. The oxygen concentration can also affect sorption and thus the availability of metal ions. If the concentration of oxygen is low (anoxic/anaerobic), microorganisms will utilise other electron acceptors for reduction for the degradation of organic matter. The temperature and the amount of organic matter available will affect the oxygen demand (Eriksson et al. 2019, pp. 213–216).

## **2.3 Effects caused by seasonality and age of landfill**

The chemical composition in a landfill can vary during the year. In a study by Ban Salem et. al (2014) the authors found that the concentration of heavy metal the draining system of a French landfill were higher in the summer compared to the autumn (except for Cd). This may be due to factors such as an increase in evaporation and a decreases in precipitation during summer, while the increased rainfall in autumn increases the leaching of metals and possible also the dilution (Ben Salem 2014). A recent study of groundwater in a Norwegian landfill by Abiriga et al. (2020) found no significant difference between spring and autumn for most variables for an active landfill, except for dissolved oxygen, sulphate and chloride, for which concentrations were higher in spring. However, for a closed landfill there was a significant difference between the seasons for almost every variable. The study also found a correlation between groundwater quality and

landfill age: while the concentration of oxygen, nitrate and sulphate increased with long age for a closed landfill, the concentration of other solutes in the study decreased (Abiriga et al. 2020).

## **2.4 PFASs**

### **2.4.1 Definition**

PFASs are substances with at least one carbon (C) atom where the hydrogen (H) atoms are replaced by fluorine (F) atoms and is thus of the form  $C_nF_{2n+1}$ - (Cheremisinoff 2016, p.9). In perfluoroalkyls, fluorine has replaced all hydrogen atoms on all carbon atoms. This does not include replacement of hydrogen which would change the functional groups. In polyfluoroalkyls, fluorine has replaced all hydrogen atoms on at least one carbon atom (Buck et al. 2011). PFASs can be divided into two groups after chain length. Long-chain PFASs are either perfluoroalkyl carboxyl acids (PFCA) with eight or more carbon atoms or perfluoroalkane sulfonates (PFSA) with six or more carbon atoms (ibid.). The reason for this different classification for the groups of substances is due to the latter being more bioaccumulative and/or inclined to bioconcentrate than the former, if substances with equal number of carbon atoms are compared (ibid.).

There are substances known as PFAS precursors, which can be transformed into different kinds of PFASs (Cheremisinoff 2016, p.18-19). N-ethyl-perfluorooctane sulfon-amido ethanol (EtFOSE) and N-methyl-perfluorooctane sulfon-amido ethanol (MeFOSE) can form PFOS through degradation through ethyl perfluorooctane sulfonamido acetic acid (EtFOSAA), perfluorooctane sulfonamido acetic acid (FOSAA) and perfluorooctane sulfonamide (FOSA) and through Methylperfluorooctane sulfonamidoacetic acid (MeFOSAA), FOSAA and FOSA, respectively (Buck et al. 2011). EtFOSE has been used in paper and packaging products (Buck et al. 2011; Rhoads et al. 2008) and different polymers of EtFOSE was used on textile surfaces (Cheremisinoff 2016), while MeFOSE has been used in the textile and carpet industry (Buck et al. 2011). All PFASs are a result of human activity and cannot be found naturally in the environment (KEMI 2022).

### **2.4.2 Production and Use**

PFASs are synthetic substances that are highly stable, even at high temperatures (Cheremisinoff 2017; ECHA n.d.). They have many desirable properties, since they are water-, fat- and dirt-repellent (Miljösamverkan Sverige 2022). Due to their dual nature of being both hydrophobic and lipophobic, they have been widely used as surfactants (Cheremisinoff 2016). Many PFASs, like PFOS, are used

in firefighting foams such as AFFFs (aqueous firefighting foams) (Cherimisinoff 2017, p.55; ECHA n.d.). Other common uses are in textiles, paper packaging, paint, ski wax, building material and more (Miljösamverkan Sverige 2022). It was around the 1950s that commercial production of PFASs began (ibid.). Due to company initiatives, restrictions and bans, the last 20 years the production of PFASs has decreased. However, in the labour of reducing the use of long-chained PFASs, the production of short-chained PFASs has increased (Lenka et al. 2021).

To produce PFASs, two methods have been used: electrochemical fluorination (ECF) and telomerization. While the ECF process forms a combination of linear and branched PFASs, the other process, telomerization, forms mainly linear PFASs. There are several different EFC processes. In the Simons process, perfluoro-1-octane sulfonyl fluoride (POSF), a C8 compound, is produced and used as a starting compound. The POSF will then, through several reactions, form MeFOSE or EtFOSE as well as several biproducts (Cheremisinoff 2016, p.11). POSF and perfluorooctanoyl fluoride are commonly used to produce PFOS and PFOA, respectively (Buck et al. 2011). Since year 2000, however, producers have shift towards the use of the C4-compound perfluorobutane in EFC to produce other types of PFASs, which are less potentially harmful, and a shift towards perfluoroalkyl C6 compounds rather than C8 in the telomerization industry (ibid.) Furthermore, polyfluorinated PFAS have replaced perfluorinated PFAS since they have a higher potential to degrade (ibid.).

### 2.4.3 PFAS in Landfills

The Swedish Environmental Protection Agency (Naturvårdsverket) list landfills as one of the most important potential sources for direct or indirect release of PFAS (Gleisner et al. 2019). Leachate from landfills can be contaminated with an abundance of different PFASs, depending on the waste that has been deposited on the landfill. The importance of leachate treatment is therefore great (ibid.). With data from Swedish landfills, Hansson et al. (2016) have estimated the yearly emission of  $\Sigma_{14}$ PFAS to WWTP to be 63 kg/ year, and to surface water to be 4.1 kg/year. For PFOS, these numbers are 3.4 and 0.2, respectively.

On landfills, different kinds of waste types are present. Landfill WWTP sludge and solid waste can be a source of PFAS, since, as stated above, PFASs have commonly been used on different types of solid material (Huset et al. 2011). Gobelius et al. (2018) has shown that the PFAS FOSA in groundwater is strongly associated with landfills/waste disposals. They also found that the distribution differed between groundwater and surface water: in groundwater, the distribution of PFSAs and PFCAs were quite similar (49% and 41%, respectively), while in surface water PFCAs were clearly dominating over PFSAs (72% and 19%,

respectively), with (PFOA and PFHxA dominating. The distribution of PFAS precursors were similar for groundwater and surface water (9.3% and 9.5%, respectively). The most abundant PFASs in landfill leachate is commonly PFCAs (Fuertes et al. 2017; Huset et al. 2011). PFASs with higher mobility in soil, such as short-chained PFASs compared to long-chained PFASs, and PFCAs compared to PFSAAs, will move faster and thus change the composition of PFAS in groundwater, while in surface waters the PFAS composition will not change as much, thus more resembling the initial composition of PFAS in leachate (Gobelius et al. 2018). Huset et al. (2011) found that short-chained PFASs was more common than long-chained PFASs in landfill leachate, which they believe to be because of short-chained PFASs preference towards an aqueous phase. After firefighting sites, landfills and waste disposals have the highest PFAS concentrations (Gobelius et al. 2018).

In a review study by Hamid et al. (2018) of landfill leachate some general patterns arise. The most common PFAS were PFCAs. Short-chained PFAS was more abundant than long-chained perfluoroalkyl acids (PFAAs), which could be linked to the shift towards short-chained PFAS (ibid.). The physio-chemistry of a landfill will vary temporally and spatially, and so the mobility and degradation of PFAS can potentially also be impacted. For example, an increase in pH have been linked to an increase in mobility of different PFASs, while the link between electrical conductivity and the mobility of PFASs does not seem univocal (ibid.).

In a study from 2022, PFAS data from Swedish landfills were compiled and PFAS concentrations and leachate treatment effectiveness were analysed. No univocal conclusion could be drawn of the leachate treatment process effectiveness. For three landfills, the concentration decreased after the treatment process while for one, the concentration of (mostly short-chained) PFAS increased. Other analyses showed little difference in concentration for the majority of PFAS before and after treatment; some PFASs increased in concentration (PFOS and 6:2 FTSA) while other decreased (PFDA) (Miljösamverkan Sverige 2022).

#### **2.4.4 PFAS Regulations**

Two of the most researched PFASs, perfluorooctane sulfonic acid (PFOS) and perfluorooctanoic acid (PFOA) are classified as Persistent Organic Pollutants (POPs) and are restricted and banned, respectively, in EU, and several others are in the process of being restricted (ECHA n.d.). PFOS is also a PBT (persistent, bioaccumulative and toxic) substance (Cheremisinoff 2016, p.13) which only degrades through combustion (ibid., p. 96). For many other PFAS, a restriction has been proposed (ECHA n.d.).

In Sweden, the recommended level of PFAS $\Sigma_{11}$  in drinking water is 90 ng/L. This value is not binding by law, but PFAS content cannot pose a risk to human health (Swedish Food Agency 2022). The Swedish Food Agency's (SFA, Livsmedelsverket) recommended level of PFAS follows European Food Safety Authority's (EFSA) health based threshold value of 4 ng/l for PFAS4 and 100 ng/l for PFAS 21. The working guideline value for PFOS in groundwater, provided by the Swedish Geotechnical Institute (Statens geotekniska institut, SGI), is 45 ng/L. The environmental quality standard value for PFAS $\Sigma_{11}$  in groundwater is also set to 90 ng/L (Swedish Chemicals Agency 2020). For inland surface waters, the limit value is legally binding in such way that if the limit value is exceeded, the Water authorities (Vattenmyndigheterna) must provide an action plan towards the environmental quality standard. The yearly mean limit value for PFOS is 0.65 ng/L and the maximum value is 36  $\mu\text{g}$  PFOS/L.

## 2.5 Statistics

There are several statistical measurements to describe a set of data. Common ways are central tendency (such as mean and median) and variability (such as standard deviation and interquartile range). For both mean and standard deviation, extreme values have a notable impact (Helsel et al. 2020).

It is rarely possible to capture a whole population in a data set, and so it is practical to describe a population from a sample. In order to determine the range between the population mean and the sample mean, the standard error of mean (SEM) can be calculated from the standard deviation (Grandin 2012):

$$SEM = \frac{s}{\sqrt{n}} = \frac{\sqrt{\frac{\sum (x_i - \bar{x})^2}{n-1}}}{\sqrt{n}}$$

Often is it relevant to know the relationship between two variables. For this, correlation can be used. However, correlation will not say anything about causality and it only works for linear relationships (ibid.). The coefficient of correlation,  $r$ , is a value between -1 and 1, where -1 indicates a negative correlation, 1 indicates a positive correlation and 0 that there is no correlation. Thus, negative correlation means that when one variable increases, the other decreases. The correlation coefficient is calculated:

$$r_{AB} = \frac{cov_{AB}}{std_A \times std_B} \quad (1)$$

The covariance ( $cov_{AB}$ ) can be calculated as follows:

$$cov = \frac{\sum(A - \bar{A})(B - \bar{B})}{n - 1} \quad (2)$$

### 2.5.1 Principal Component Analysis

Multivariate statistical methods are common tools to investigate groundwater character and to characterise contamination sources and transportation in time and space (Gu et al. 2015). There are many types of multivariate methods, including factor analysis, principal component analysis (PCA), cluster analysis, and discriminant analysis.

A PCA is a statistical tool to reduce multi-dimensional data into lower dimensions, which are easier to present, without losing valuable information about the variance (Jolliffe and Cadima 2016). Essentially, this is achieved by creating variables that are linear functions of the ones of the original data set, called principal components (PCs), which are orthogonal and uncorrelated. The idea is to have most of the variation in the first PCs (Olsen et al. 2012).

The observations of different variables  $p$  for the observations  $n$  are arranged in a matrix which is used to find the covariance or correlation matrix. The different variables for all observations are ordered in a  $n \times p$ -sized matrix, denoted  $\mathbf{X}$  in Jolliffe and Cadima (2016). The maximum variance of the linear combination of  $\mathbf{X}$  with the constants  $\mathbf{a}$  is obtained from the sample covariance matrix  $\mathbf{S}$ , which consists of the covariance for every variable pairs. In other words,

$$var(\mathbf{Xa}) = \mathbf{a}^T \mathbf{S} \mathbf{a}$$

This equation becomes a maximation problem (for further details, see Jolliffe and Cadima (ibid.)) and can be solved as

$$\mathbf{S} \mathbf{a} = \lambda \mathbf{a},$$

where  $\mathbf{a}$  is an eigenvector and  $\lambda$  is the eigenvalue of  $\mathbf{S}$ , where the values of the latter are the variance (ibid.). The eigenvectors are called *PC loadings* (ibid.) and describe how much each variable contributes to a PC (Helena et al. 2000). From the eigenvectors of the covariance matrix the *PC scores* can be retrieved from the new linear combination  $\mathbf{Xa}_k$  ( $k=1,2,\dots,p$ ) (Jolliffe and Cadima 2016).

A PCA can also be explained in a geometrical way. The  $n$  observations of  $p$  variables can be conceived as  $n$  points in a  $p$ -dimensional space. The principal component is then a  $p$ -dimensional hyperplane fitted through these points with

the minimal least squares method (Wold et al. 1987). Fig. 1 shows an example in a 3-dimensional space, where the PC is a line.

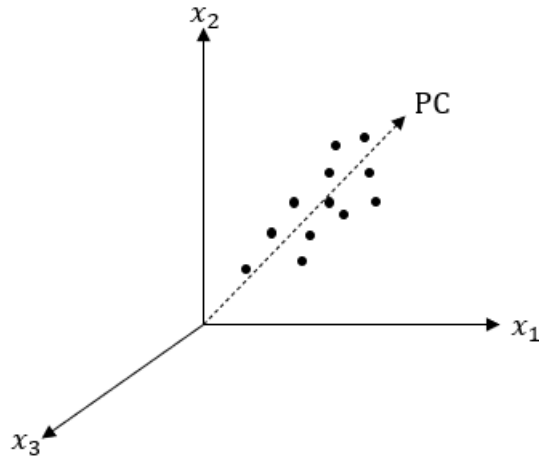


Figure 1: An example of a principle component in a 3-dimensional space. The (feigned) data set has been approximated with one PC. After Wold et al. (1987).

A PCA can be done using either a correlation or a covariance matrix. The advantage with correlation is that it is easier to compare variables. The disadvantage with covariance PCAs is that variables ought to have the same units, otherwise large variances in some variables may dominate the PCs (Jolliffe 1986, p. 17). However, fewer PCs are needed for a covariance matrix compared to a correlation matrix to present an equally large part of the total variance (Jolliffe and Cadima 2016). It is common to first standardize the variables (i.e. mean=0 and std=1) to avoid problems arising if the variables have different units, since variance is dependent on unit. The standardized matrix is the same as a correlation matrix (ibid.).

### 2.5.2 Interpreting PCA plots

A PCA is a very good way to visualise high-dimensional data. There are two common ways to present PCA data: a *score plot* and a *biplot*.

A *score plot* describes the value an observation would have for a certain PC (ibid.). The closer the points are to the center of the plot, the closer their value are to the mean value and the closer the points are to each other, the more similar they are (Hartmann et al. 2018).

A *biplot* is a practical tool since it captures both the scores and the loadings. The loading vectors represents the original variables, and so the more a variable contributes to a principal component, the closer the loading vector will be to the PC, i.e the angle between them will be smaller. The longer the loading vector is, the more of its variability is captured by the two PCs (Hartmann et al. 2018). Conclusions can not only be drawn from the relationship between the loading vectors and the displayed principle components, but also from the relationship of the loading vectors between each other. The closer the loading vectors are (i.e the smaller angle), the more positive correlation they have and the further away from each other they point, the more negative the correlation is. Perpendicular loading vectors are not correlated (ibid.).

### **2.5.3 Addressing Missing Values**

An important part of the PCA is addressing missing values. If there are few missing values a possibility is to simply exclude that individual or variable from the analysis. However, discarding a whole individual or variable due to one missing observation is an undesirable loss of information (Dray and Josse 2015). There are three common solutions to this problem. The first is to replace the missing value with a presumptive value, such as the mean. The drawback with this is that it will alter the dataset; the variance decreases and the correlation within the data set changes (Little and Rubin (2002) via Dray and Josse (ibid.)). Nevertheless, it can be useful for some missing values. Another method is to, before performing the PCA, alternate the PCA, so that it can operate without the missing values. Lastly, a PCA can be used to estimate the missing value through iteration (ibid.).

## **3 Method and Material**

### **3.1 Hovgården waste facility**

#### **3.1.1 Site description**

Today Hovgården serves several purposes: as a recycling facility for the public, as a place for sorting and interim storage for waste (such as residues from digested sewage sludge, wood waste and combustible waste for incineration), treatment of contaminated soils, as a compost and as an active landfill. The sorting, interim storage and composting is performed on six impervious surfaces (Uppsala Vatten 2020). Today, Hovgården accepts 94 000 tonnes of waste every year. The types of waste includes contaminated soils, compost, sorted material from building sites, asbestos and other industrial waste. The waste fractions have different fates: 18% of the waste is reused on site as construction material, while approximately 12 % are deposited on the landfill (mostly insulation and plaster) (Uppsala Vatten 2021). The actual landfill can be divided into two parts; on the "old landfill" (Etapp 1) where hazardous waste was deposited. Depositing ended in 2016 and in 2019 it was sealed with a final cover. Organic waste has not been deposited on Hovgården. The "active landfill" (Etapp 2) is still running and only non-hazardous waste is deposited. The facility has its own WWTP combined with several ponds, where leachate water from the area is treated. The total area of Hovgården is 570000 m<sup>2</sup> (57 ha<sup>2</sup>) (Bonnet 2018).



Figure 2: Hovgården waste facility. Photo by Uppsala Vatten och Avfall 2020-06-01.

### 3.1.2 Hovgården wastewater treatment

Leachate from a landfill can contain various types of contaminants and nutrients, which poses a risk if leached to the environment and thus needs to be treated (Uppsala Vatten och Avfall AB n.d.). The leachate from the facility is collected in a drainage system in the bottom of the landfill and from the six impervious surfaces used for composting and storage of the compost product, and from the sorting of waste. The majority of the wastewater is pumped directly to the wastewater treatment plant. The current WWTP has been operating since around 2007 (Uppsala Vatten 2020). In the WWTP the water is treated in several steps (Fig. 3). First, leachate is mechanically treated by aeration, which oxidizes iron, manganese, and organic substances, followed by a lamella sedimentation where the compounds are removed through sedimentation. In the biological step, ammonium is oxidized and organic substances are degraded. A moving bed biofilm reactor (MBBR) provides a surface on which the microbes can grow. In the next step, phosphorus is precipitated with a coagulant, consisting of aluminum chloride, and a polymer. Lastly, the water is transferred to first a sedimentation pond and then to two polishing ponds. Before entering the recipient Hovgårdsbäcken, the water is aired in an aeration pond (ibid.). The point where wastewater enters the WWTP is referred

to as R1, the point before the biological treatment step as R2 and the WWTP outlet, where the treated wastewater leaves the WWTP in two different conduits, are referred to as R3 and R4, respectively.

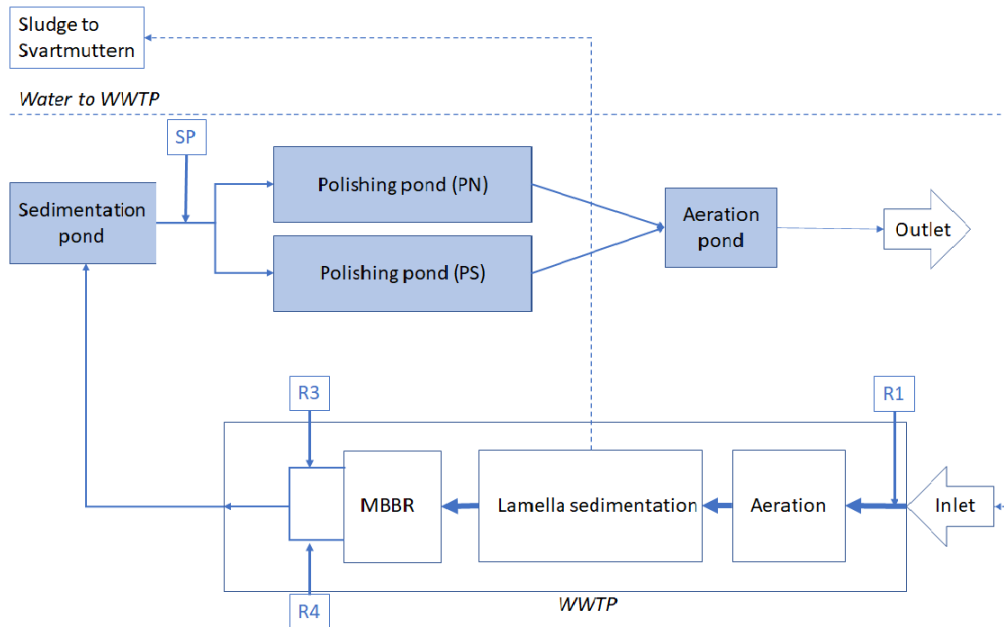


Figure 3: Wastewater flow in the WWTP in Hovgården. MBBR = moving bed biofilm reactor; Sampling points R1-R3 (WWTP), SP (sedimentation pond), and Polishing ponds (PN and PS).

The leachate from the sludge cell are treated in a few extra sedimentation steps before entering the WWTP.

### 3.1.3 The polishing ponds

The polishing ponds (Fig. 4) are situated in the eastern part of Hovgården facility. This is the the last step of the wastewater treatment process, before the water is aired in the aeration pond and exits the facility. The northern pond (PN) is approximately 170 m long and 18 m wide in average. The depth was approximately 1,5 m in the beginning and in the middle of the pond and 1,73 m in the end of the pond when measured in December 2020. The southern pond (PS) is approximately 150 m long and 19 m wide in average. The depth was approximately 1,4 m in the pond in December 2020. The bottom sediment levels were low in PN while high in PS in December 2020. The total surface and the total volume of each pond is 7 000 m<sup>2</sup> and 10 000 m<sup>3</sup>, respectively. The retention time for the

dimensioning water flow  $Q_{dim}$  is  $\sim 8.3$  days in both ponds, however a recent trial has indicated otherwise and that the flow to PN is actually higher than that to PS. The polishing ponds used to be one large pond, but was converted likely in the 90s to their current dual state.

Along the northern side of PN run several water pipes, leading leachate to the WWTP and sludge from the WWTP to Svartmuttern. There is also a pipe that can be used to relocate wastewater from the sedimentation pond, past the polishing ponds to the outlet, in case of failure in the ordinary pipes.

As Fig. 4 shows, PS is situated closer to the forest and is therefore more shadowed than PN. The vegetation in the ponds differ; in PN there are more surface growth while in PS there are more macrophytes.



Figure 4: The polishing ponds. PN is situated to the right in the figure and PS to the left. Photo by Uppsala Vatten och Avfall **2020-06-01**

### 3.2 Hydrogeological Survey

Hovgården is situated in a valley directed east-west in Uppsala municipality. The level of the valley was originally between 30 meters above mean sea level (mamsl) (in east) and 35 mamsl (in west) (Golder 2004), however this has been modified by the landfill and of 2020 the highest mamsl is + 77.7 m (Uppsala Vatten 2020).

North and south of the landfill the mamsl is +50 m and +48 m, respectively. The total area of the watershed of Hovgården was 55 ha in year 2004 (Golder 2004). The groundwater flow is generally from higher grounds of the landfill in the west and the runoff flows to the east (ibid.). The bottom of the landfill is not artificially sealed but sealed naturally by a clay layer (ibid.). Three water-bearing fracture zones have been found in the bedrock under the landfill (ibid.).

There are several groundwater wells in the area (Fig. 5). Southwest of the landfill is the well 18G02, which is presumed to be unaffected by the landfill. P6 and P8 are located at Svartmuttern and 18G09 and 18G10 are located on the active landfill. P3 INSIDA and P3 UTSIDA (in this thesis also called P3 IN and P3 UT, respectively) are located east of the active landfill. In 1996 a barrier was constructed downstream the landfill to prevent the transport of contaminated groundwater. The wells P3 INSIDA and P3 UTSIDA were installed on the in- and outside of the barrier (Bjälkefur Seroka, S., personal communication, 2023-01-16). H1C and 18G12 are located in the northeast of the landfill, while P1 and P2 are located in the southwest and south of Hovgården, respectively. Close to the east border, where the treated wastewater leaves the facility, P24 is located. The well 18G14 is a very deep bedrock well, thus representing a different kind of groundwater than that on the landfill in general.



Figure 5: Map over Hovgården groundwater wells. Figure by Sofia Seroka Bjälkefur. Used with permission.

### 3.3 Sampling and Field Measurement

#### 3.3.1 Groundwater wells

The wells were sampled and field measurements were performed three times. Before sampling, the wells were purged with three well volumes (3). If this was not possible due to a low recovery rate, the wells were purged at least one time. Some wells were purged the day before, due to the limited time of the day of the sampling.

$$RV = l_{well} \times (d_{well}/2)^2 \quad (3)$$

For every well, an individual tube was used, to reduce the risk of contamination. Water was collected in plastic flasks for analysis and in a plastic litre measure, where field measurements of pH, conductivity, temperature and oxygen were performed with a Hach HQ2200 Portable Multi-Meter.



Figure 6: Sampling of groundwater wells in February. Photo by the author (2022-02-09).

### 3.3.2 The polishing ponds

The polishing ponds (PS and PN) were sampled at 3 occasions, in February 23, March 15 and May 2nd, 2022, and samples were collected in plastic bottles. There were a total of 6 sampling points in each pond (Fig. 7)

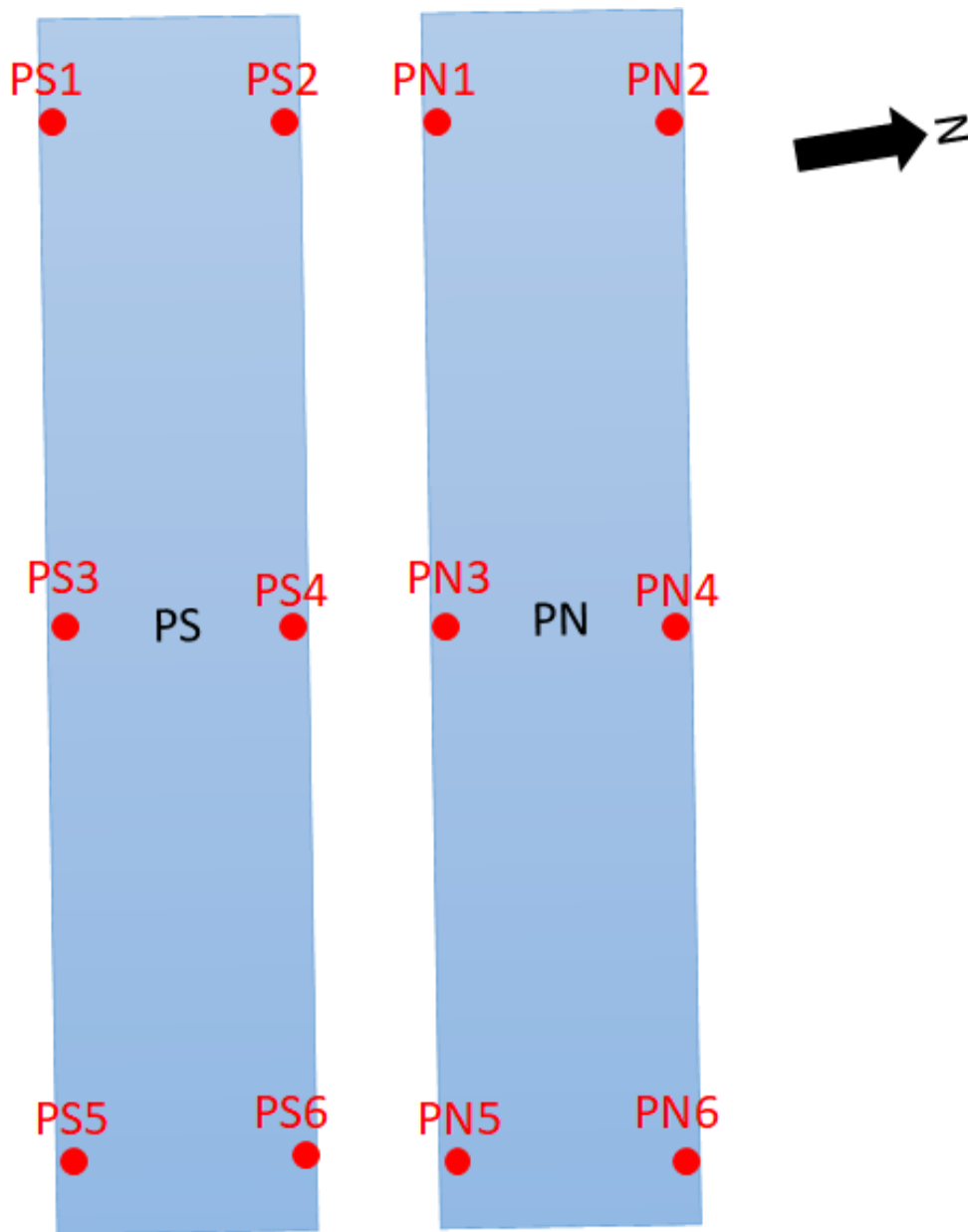


Figure 7: Sampling points in the polishing ponds. The figure is not according to scale. This is a schematic figure and not the actual shape of the ponds.

When sampled the first time (2022-02-23), the surfaces of the ponds were frozen. Holes were drilled in the ice and the sample was taken from the surface water. Field measurements were performed in the litre measure (2022-02-23) and directly in the ponds (2022-03-07). The second time the polishing ponds were sam-

pled (2022-03-21), they were still partly frozen and thus some samples were taken in drilled holes in the ice (PS1, PS3, PS5 and PS6) while the rest of the samples were sampled with a pump.



Figure 8: Sampling of the polishing ponds. Photo by the author **2022-05-02**.

Due to the sedimentation pond being dredged in the middle of April, the last sampling occasion was postponed to 2022-05-02, to avoid contamination from the dredging. Sampling of the sedimentation pond as well as the WWTP (R1, R3 and R4) was not a part of this project, but available data from an earlier sampling occasions was used in order to facilitate interpreting polishing pond data. The sedimentation pond was then sampled in the outlet of the pond. Due to the small size of the sedimentation pond, a leakage into the sedimentation pond was not considered in this study.

Table 1: Compiled information of all samples. The different water types are abbreviated: PP stands for polishing ponds, WWTP is wastewater treatment plant and GRW is groundwater. M stands for metals, FP for field parameters and Mi for micro ions. For samples noted \* no data existed for Alk, NO<sub>3</sub><sup>-</sup>, Cl and SO<sub>4</sub>. For samples noted \*\*, no data existed for NO<sub>3</sub>, Cl and SO<sub>4</sub>. For samples noted \*\*\* no data existed for O<sub>2</sub> and lastly, for samples noted \*\*\*\* no data existed for O<sub>2</sub> or temp.

<b>Sampling information</b>			
ID	Date	Water type	Type
PN1	2021-09-02	PP	M
PN2	2021-09-02	PP	M
PS1	2021-09-07	PP	M
PS2	2021-09-07	PP	M
PS_in	2021-11-24	PP	FP, M, Mi
PS_mitt	2021-11-24	PP	FP, M, Mi
PS_in	2021-12-15	PP	FP, M, Mi
PS_mitt	2021-12-15	PP	FP, M, Mi
PN_in	2021-12-15	PP	FP, M, Mi
PN_mitt	2021-12-15	PP	FP, M, Mi
PS1	2022-02-23	PP	FP, M, Mi
PS2	2022-02-23	PP	FP, M, Mi
PS3	2022-02-23	PP	FP, M, Mi
PS4	2022-02-23	PP	FP, M, Mi
PS5	2022-02-23	PP	FP, M, Mi
PS6	2022-02-23	PP	FP, M, Mi
PN1	2022-02-23	PP	FP, M, Mi
PN2	2022-02-23	PP	FP, M, Mi
PN3	2022-02-23	PP	FP, M, Mi
PN4	2022-02-23	PP	FP, M, Mi
PN5	2022-02-23	PP	FP, M, Mi
PN6	2022-02-23	PP	FP, M, Mi
PS1	2022-03-21	PP	PFAS, FP, M, Mi*
PS2	2022-03-21	PP	PFAS, FP, M, Mi*
PS3	2022-03-21	PP	PFAS, FP, M, Mi*
PS4	2022-03-21	PP	PFAS, FP, M, Mi*
PS5	2022-03-21	PP	PFAS, FP, M, Mi*
PS6	2022-03-21	PP	PFAS, FP, M, Mi*
PN1	2022-03-21	PP	PFAS, FP, M, Mi*

PN2	2022-03-21	PP	PFAS, FP, M, Mi*
PN3	2022-03-21	PP	PFAS, FP, M, Mi*
PN4	2022-03-21	PP	PFAS, FP, M, Mi*
PN5	2022-03-21	PP	PFAS, FP, M, Mi*
PN6	2022-03-21	PP	PFAS, FP, M, Mi*
PS1	2022-05-03	PP	FP, M, Mi
PS2	2022-05-03	PP	FP, M, Mi
PS3	2022-05-03	PP	FP, M, Mi
PS4	2022-05-03	PP	FP, M, Mi
PS5	2022-05-03	PP	FP, M, Mi
PS6	2022-05-03	PP	FP, M, Mi
PN1	2022-05-03	PP	FP, M, Mi
PN2	2022-05-03	PP	FP, M, Mi
PN3	2022-05-03	PP	FP, M, Mi
PN4	2022-05-03	PP	FP, M, Mi
PN5	2022-05-03	PP	FP, M, Mi
PN6	2022-05-03	PP	FP, M, Mi
R1	2022-03-02	WWTP	PFAS
R3	2022-03-02	WWTP	PFAS
R4	2022-03-02	WWTP	PFAS
SP	2022-03-02	SP	PFAS
P1	2021-02-03	GRW	M, Mi**
P2	2021-02-03	GRW	M, Mi**
P3 IN	2021-02-03	GRW	M, Mi**
P3 UT	2021-02-03	GRW	M, Mi**
P6	2021-02-03	GRW	M, Mi**
P8	2021-02-03	GRW	M, Mi**
P24	2021-02-03	GRW	M, Mi**
P1	2021-09-15	GRW	FP, M, Mi***
P2	2021-09-15	GRW	FP, M, Mi***
P3 IN	2021-09-15	GRW	FP, M, Mi***
P3 UT	2021-09-15	GRW	FP, M, Mi***
P6	2021-09-15	GRW	FP, M, Mi***
P8	2021-09-15	GRW	FP, M, Mi***
P24	2021-09-15	GRW	FP, M, Mi***
P1	2021-11-17	GRW	PFAS, FP, M, Mi****
P2	2021-11-17	GRW	PFAS, FP, M, Mi****
P3 IN	2021-11-17	GRW	PFAS, FP, M, Mi****

P3 UT	2021-11-17	GRW	PFAS, FP, M, Mi****
P6	2021-11-17	GRW	PFAS, FP, M, Mi****
P8	2021-11-17	GRW	PFAS, FP, M, Mi****
P24	2021-11-17	GRW	PFAS, FP, M, Mi****
18G02	2021-11-17	GRW	PFAS, FP, M, Mi****
P1	2022-02-09	GRW	FP, M, Mi
P2	2022-02-09	GRW	FP, M, Mi
P3 IN	2022-02-09	GRW	FP, M, Mi
P3 UT	2022-02-09	GRW	FP, M, Mi
P6	2022-02-09	GRW	FP, M, Mi
P8	2022-02-09	GRW	FP, M, Mi
P24	2022-02-09	GRW	FP, M, Mi
18G02	2022-02-09	GRW	FP, M, Mi
18G09	2022-02-09	GRW	FP, M, Mi
18G10	2022-02-09	GRW	FP, M, Mi
H1C	2022-02-09	GRW	FP, M, Mi
18G12	2022-02-09	GRW	FP, M, Mi
18G12	2022-03-15	GRW	PFAS, FP, M, Mi
H1C	2022-03-15	GRW	PFAS, FP, M, Mi
P3 IN	2022-03-15	GRW	PFAS, FP, M, Mi
P3 UT	2022-03-15	GRW	PFAS, FP, M, Mi
18G09	2022-03-15	GRW	PFAS, FP, M, Mi
18G02	2022-03-15	GRW	PFAS, FP, M, Mi
P1	2022-06-08	GRW	PFAS, FP, M, Mi
P2	2022-06-08	GRW	PFAS, FP, M, Mi
P3 IN	2022-06-08	GRW	PFAS, FP, M, Mi
P3 UT	2022-06-08	GRW	PFAS, FP, M, Mi
P6	2022-06-08	GRW	PFAS, FP, M, Mi
P8	2022-06-08	GRW	PFAS, FP, M, Mi
P24	2022-06-08	GRW	PFAS, FP, M, Mi
18G02	2022-06-08	GRW	PFAS, FP, M, Mi
18G14	2022-06-08	GRW	PFAS, FP, M, Mi

### 3.4 Sample analysis

Metal and PFAS analysis was performed by ALS Scandinavia AB. Analysis of other parameters (alkalinity, ammonium as nitrogen (NH<sub>4</sub>-N), nitrite as nitrogen (NO<sub>2</sub>-N) and total nitrogen (N-tot)) was performed by Uppsala Vatten's own laboratory. The individual PFASs included in the analysis were PFBA, PFPeA,

PFHxA, PFHpA, PFOA, PFNA, PFDA, PFBA, PFHxS, PFOS, 6:2 FTS, PFAS $\Sigma_{11}$ , PFUnDA, PFDoDA, PFTrDA, PFTeDA, PFPeS, PFHpS, PFNS, PFDS, PFDoDS, 4:2 FTS, 8:2 FTS, FOSA, MeFOSA, EtFOSA, MeFOSE, EtFOSE, FOSAA, MeFOSAA, EtFOSAA, HPFHpA and PF37DMOA (Table 7).

### 3.5 Data Treatment

Data was compiled in a matrix in Excel. Based on Olsen et al. (2012), samples under the detection limit was set to half the detection limit. If more than 50 % of all the samples were below the detection limit, the variable was excluded from the analysis. These modified samples were used in statistical analysis. For plotting fractional distribution and concentrations, values under the detection limit was set to zero. The Excel standard error was used to show sample variability.

A correlation analysis with Pearson's method was performed in R (Version 4.1.2) for both groundwater and surface water for PFAS, and groundwater and polishing pond data separately for metal and macro ion data.

### 3.6 Flow and Mass Balance

The first part of this study was to investigate the suspicion that there is a flow of contaminating groundwater to the polishing ponds. This task was split in two parts, where the the first part was to investigate if there is an additional unknown flow to the ponds, and if so, if this flow has an impact on the water quality of the ponds.

First, flow data for WWTP inflow (R1) and outflow (A1) was retrieved. From the WWTP, sludge from the lamella sedimentation is diverted to Svartmuttern through pumping. The pump runs for two minutes, and then rests for 60 min. Hence, the pumping cycle is 62 minutes. The pumping rate was estimated using the bucket method (not as a part of this study) and was approximately 5 L/s. In 24 h, the pump runs 23.2 cycles, which gives a daily sludge flow of 13.9 m<sup>3</sup>/day (Appendix A.1). This flow was then subtracted from the daily flow through R1, and this modified flow was assumed to be the WWTP outflow. This outflow was assumed to be the inflow to the polishing ponds. Inflow and outflow data was compared in order to analyse if the outflow was greater than the inflow, which should mean that there is an unknown flow contributing to the outflow.

To confirm the suspicion that there is a mass flow to the ponds, a mass balance was performed. Wastewater concentration data was collected from R3 and R4, which are outlet of the two parallel lines in the biostep and represents the last sampling point before the treated wastewater enters the sedimentation pond, and

the average concentration in these two points was calculated (henceforth called R34). This concentration represented the concentration in the polishing ponds inflow. The outflow concentration and flow data was taken after the aeration pond in A1, right before the treated wastewater empties into the recipient. The mass flow was calculated as the flow times the concentration:

$$Q_m = Q \times c$$

The difference between R34 and A1 in mass flow per month was calculated. From the monthly difference in flow and the mass flow, the concentration of the unknown stream was calculated as mg/L or  $\mu\text{g/L}$ .

### 3.7 Charge Balance

A charge balance was performed on macro-ions to further analyse the water chemistry and the importance of heavy metals. Groundwater data and the polishing ponds were analysed. For the polishing ponds, an average of all six sampling points in each pond were used. Concentration data in mg/l was converted to mmol/l (Eq. 3.7).

$$c[\text{mmol/l}] = 1000 \times \frac{m[\text{mg/l}] \times 10^{-3}}{M[\text{g/mol}]}$$

The macro-ions included in the charge balance were sodium ( $\text{Na}^+$ ), potassium ( $\text{K}^+$ ), calcium ( $\text{Ca}^{2+}$ ), magnesium ( $\text{Mg}^{2+}$ ), manganese ( $\text{Mn}^{2+}$ ), nitrate ( $\text{NO}_3^-$ ), chloride ( $\text{Cl}^-$ ), sulphate ( $\text{SO}_4^{2-}$ ) and hydrogen carbonate ( $\text{HCO}_3^-$ , as alkalinity) (Eq. 3.7).

$$q = [\text{Na}^+] + [\text{K}^+] + [2\text{Ca}^{2+}] + [2\text{Mg}^{2+}] + [2\text{Mn}^{2+}] - [\text{NO}_3^-] - [\text{Cl}^-] - [\text{HCO}_3^-] - 2[\text{SO}_4^{2-}]$$

### 3.8 PFAS Fingerprinting

The groundwater wells P1, P2, P3 IN, P3 UT, P6, P8, P24 and 18G02 were sampled 2021-11-17 and P3 IN, P3 UT, 18G02, 18G09, 18G12 and H1C 2022-03-15. 18G10 was not sampled due to scarcity of water. Samples from the wastewater treatment process (R1, R3, R4 and SP) were taken 2022-03-02. Samples from 2021-11-17 and 2022-03-02 were not performed in this study but by Uppsala Vatten och Avfall AB. The polishing ponds were sampled 2022-03-21. The samples

were sent to the lab and 32 different PFASs were analysed for (Appendix 7). Samples from both November 2021, March 2022 and June 2022 was considered in the analysis for P3 IN, P3 UT and 18G02, to evaluate if it was reasonable to compare November values with March values.

If samples were below the detection limit, the value was set to half of the detection limit if  $\geq 50\%$  of the samples for the PFAS substance was detected. The total concentration ( $\mu\text{g/L}$ ) of PFAS in each sample was calculated and the percentage of the total concentration was calculated for each PFAS substance. This data was then analysed in R. Since all variables (PFASs) had the same unit (%), a covariance matrix was used in the analysis. In R, *prcomp* was used to perform the PCA, and data was centered and scaled. All variables with missing values were excluded from the PCA, and ultimately PFBA, PFPeA, PFHxA, PFHpA, PFOA, PFBS, PFHxS, PFOS and PFPeS were included in the analysis.

### **3.9 PCA for ions and other statistical parameters**

A PCA was also performed for metals and macro ions, for both polishing ponds and groundwater. For groundwater, samples from February, September and November 2021 and from February, March and June 2022 were used in the analysis, and for the polishing ponds, samples from February, March and June 2022 were used (Table 1). If samples were below the detection limit, the value was set to half of the detection limit if  $\geq 50\%$  of the samples for the variable was detected. If the variable had missing values, it was excluded from the analysis. Log data was used and *prcomp* in R was used to perform the PCA, and data was centered and scaled. The variables that were included in the PCA can be found in the biplot as loading vectors.

## **4 Results**

### **4.1 Polishing Ponds Analyses**

#### **4.1.1 Polishing pond water quality**

For water quality parameters in the pond, samples from autumn, winter and spring 2021-2022 were analysed (Table 1). No samples from the summer months (June, July and August) were taken. Mean water temperature was 4.9°C and mean conductivity was 284 mS/m at °C. Max conductivity was measured in PN in March 2022 and was 417 mS/m at 25°C. The mean pH for PN and PS was 7.4 and therefore quite neutral, mean oxygen was 9.33 mg/L and mean alkalinity was 454 mg/L. For all these parameters, the mean value was higher in PN than in PS, however not always for the individual sampling occasions.

#### **4.1.2 Water and Mass Flow**

There is a clear addition of water from an unknown flow to the polishing ponds. The mean inflow to the polishing ponds from Mars 1st 2021 to January 31st 2022 was 238 m<sup>3</sup>/day and the mean outflow from A1 was 635 m<sup>3</sup>/day (Fig. 9). The water level in the ponds is not known to have been changed during this time.

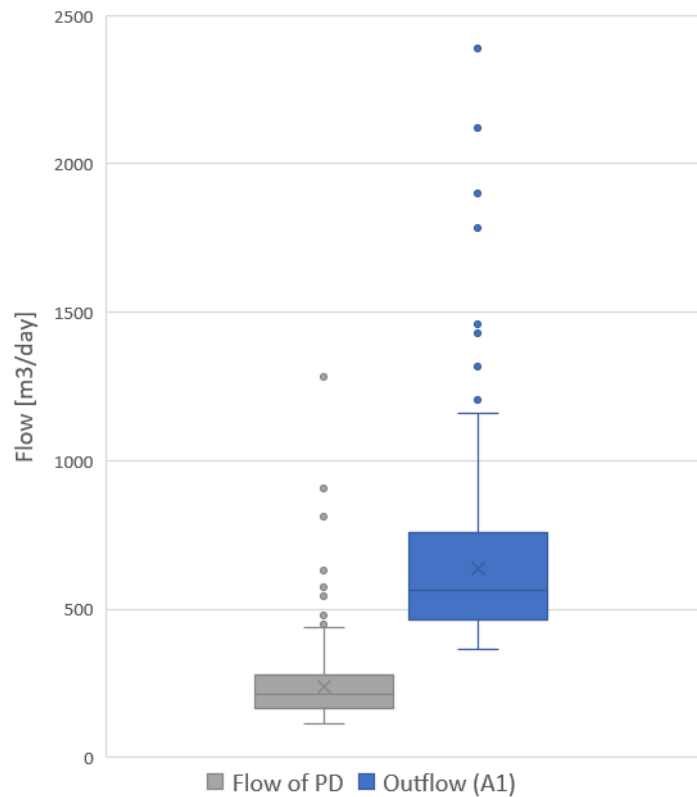


Figure 9: The mean inflow to the ponds and outflow from sampling point A1. The daily data is from 1st of March 2021 to 31st of January 2022.

The unknown inflow to the polishing ponds results in a considerable addition of ions to the ponds. There is an inflow of almost all ions (Table 2). The only exception is for chromium, iron and manganese. Especially great is the unknown mass flow of chloride, sodium, sulphate, calcium and potassium. To put this into perspective, the monthly massflow was compared to the ratio between the outflow and inflow. Then, the biggest increase in mass is for aluminum. This is probably due to aluminum chloride being used in the wastewater treatment process. There is a distinct increase in some heavy metals, most prominent copper, antimony and zinc. The quantity of ammonium and sulphate was also clearly increasing in the ponds.

Table 2: Mean mass flow to the ponds from an unknown stream from March to December 2021. The increase mass flow comparing the inflow with the outflow. Positive values indicates that mass is added to the polishing ponds<sup>a)</sup>.

	Difference in mass flow between outflow and inflow	Increase comparing the inflow and outflow
	[kg/month]	[%]
PO4	0.056	138
NH4	11.7	327
TotN	361	192
Cl	7930	209
SO4	2217	317
TOC	309	220
Al	2.68	1577
As	0.011	215
Ba	0.509	128
Ca	1230	254
Cd	0.000387	177
Co	0.00720	171
Cr	-0.0228	64.3
Cu	0.427	521
Fe	-8.90	13.2
K	1355	191
Mg	3623	201
Mn	-3.54E-06	173
Mo	0.0446	271
Na	3948	194
Ni	0.0886	206
Pb	0.00358	66.5
S	729	293
Sb	0.0213	468
V	0.00729	158
Zn	0.314	358

<sup>a)</sup> For March to December 2021 for phosphate as phosphorous, ammonium as nitrogen, total nitrogen, chloride, sulphate and TOC and for March, June, September and December for all other ions. For April for phosphate as phosphorous and December for cadmium and lead, the value fell

under the detection limit and was thus not included.

Mass flow of  $\Sigma_{11}$ PFAS was calculated and compared. There was an ostensible increase of the sum of PFAS between inflow and outflow of the polishing ponds for the sum of PFAS, where the outflow exceeds the inflow (Fig. 10). This might be due to an unknown groundwater source or the degradation of PFAS precursors to PFAAs.

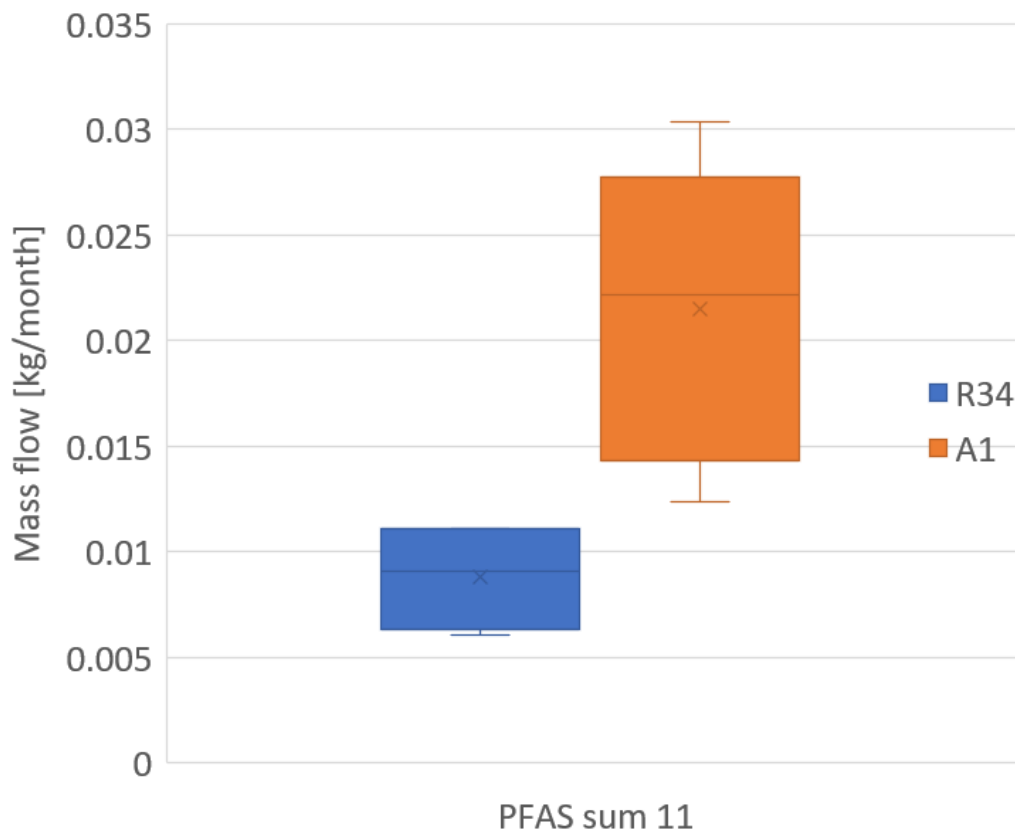


Figure 10: Monthly mass flow of PFAS. Data is from March, June, September and December 2021 for the inflow and from April, June, August, October and December 2021 for the outflow.

The concentration of the unknown flow was of the same order of magnitude as the inflow and outflow (Table 3). The concentration of aluminum, copper, antimony and zinc was higher in this unknown flow, compared to R34 and A1. Again, the chloride and aluminum concentration can probably be explained by the WWTP process, where aluminum chloride is added as a flocculant. The concentration of macro ions (e.g. Na, Cl, Ca etc.) was generally lower in the unknown inflow than

at site R34 and A1.

Table 3: The calculated concentration in the potential impact of an unknown source to the flow between R34 and A1. Negative concentrations (marked in blue) indicate that the inflow of the substance to the pond exceeds the outflow, and thus is not really a true concentration. These chemicals thus settle in the polishing ponds. The difference in concentrations between R34 and A1 were calculated as the difference in mass flow per month divided by the difference in water flow per month.

	Unit	R34	A1	Difference between R34 and A1
PO4	mg/L	0.0450	0.02	0.00457
NH4	mg/L	0.311	1.50	0.962
Tot N	mg/L	54.8	40.4	29.6
Cl	mg/L	1130	825	652
SO4	mg/L	162	182	182
TOC	mg/L	36.6	30.7	25.4
Al	µg/L	28.2	140	220
As	µg/L	1.52	1.19	0.906
Ba	µg/L	428	204	41.8
Ca	mg/L	136	123	101
Co	µg/L	1.49	0.962	0.592
Cr	µg/L	5.66	0.897	-1.88
Cu	µg/L	15.8	29.5	35.1
Fe	mg/L	1.17	0.0417	-0.731
K	mg/L	241	174	111
Mg	mg/L	57.6	43.6	29.8
Mn	µg/L	86.8	35.5	-0.000291
Mo	µg/L	4.06	4.05	3.67
Na	mg/L	690	503	324
Ni	µg/L	14.1	10.2	7.28
S	mg/L	59.1	63.7	59.9
Sb	µg/L	0.918	1.50	1.75
V	µg/L	0.745	0.438	0.599
Zn	µg/L	17.7	22.7	25.8

### 4.1.3 Macro ion distribution

The macro ion distribution were quite similar between both ponds (Fig. 11a and Fig. 11b) and between February and May (Fig. 11 and Fig. 34). Chloride and hydrogencarbonate made up around 50%, sodium around 20% and the rest of calcium, potassium, nitrate, sulphate and magnesium. There are no evident differences in macro ion distribution between the ponds; chloride and nitrate are slightly more dominating in PN compared to PS, while sulphate is slightly more dominating in PS.

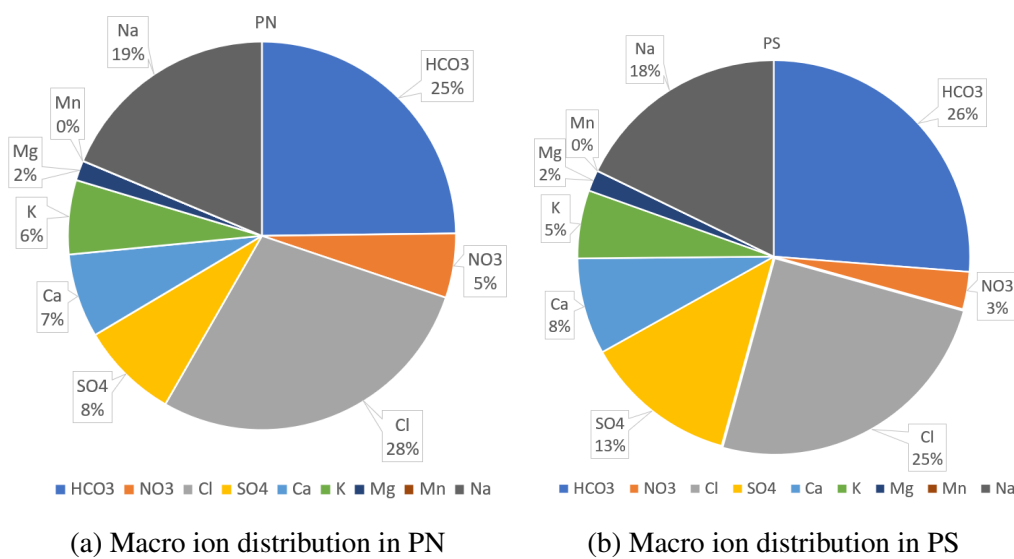


Figure 11: Macro ion distribution in the polishing ponds in February 23rd, 2022.

The sedimentation pond outlet has a similar distribution of macro ions as the polishing ponds (Fig. 11). Chloride and nitrate were somewhat greater in the sedimentation pond than in PS and PN, while sulphate and calcium were lower. The sedimentation pond was sampled on March 1st, a week after the polishing ponds.

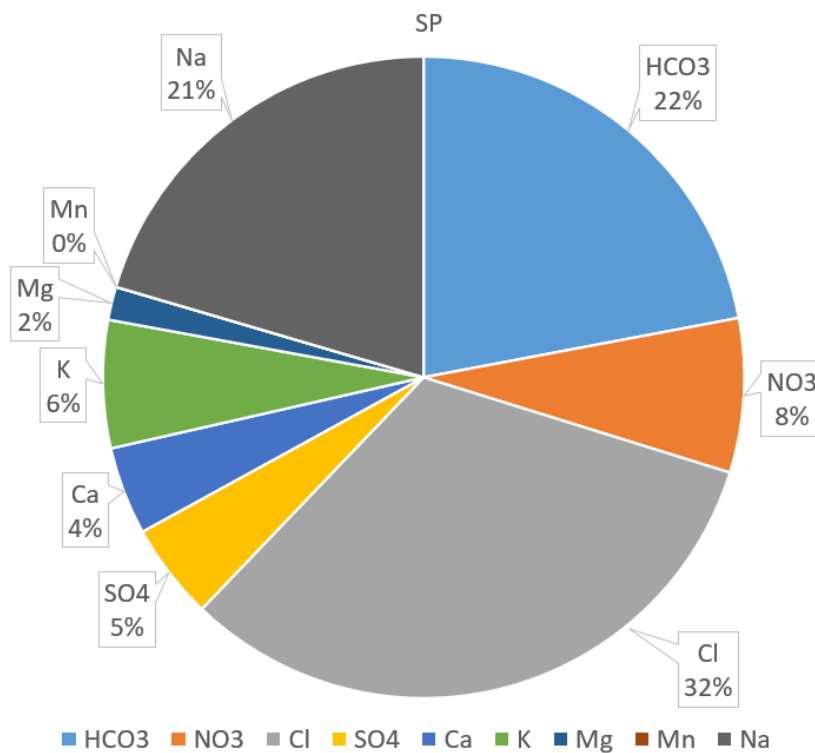


Figure 12: Macro ion distribution in the sedimentation pond in March 1st, 2022.

Comparing PN and PS, the concentration of sulphate, calcium and manganese were higher in PS, as well as iron, phosphorous and sulphur. Nitrate, chloride, potassium, magnesium, sodium and silica were higher in PN (Fig. 13). However, the different concentration of several samples falls inside the standard error bars.

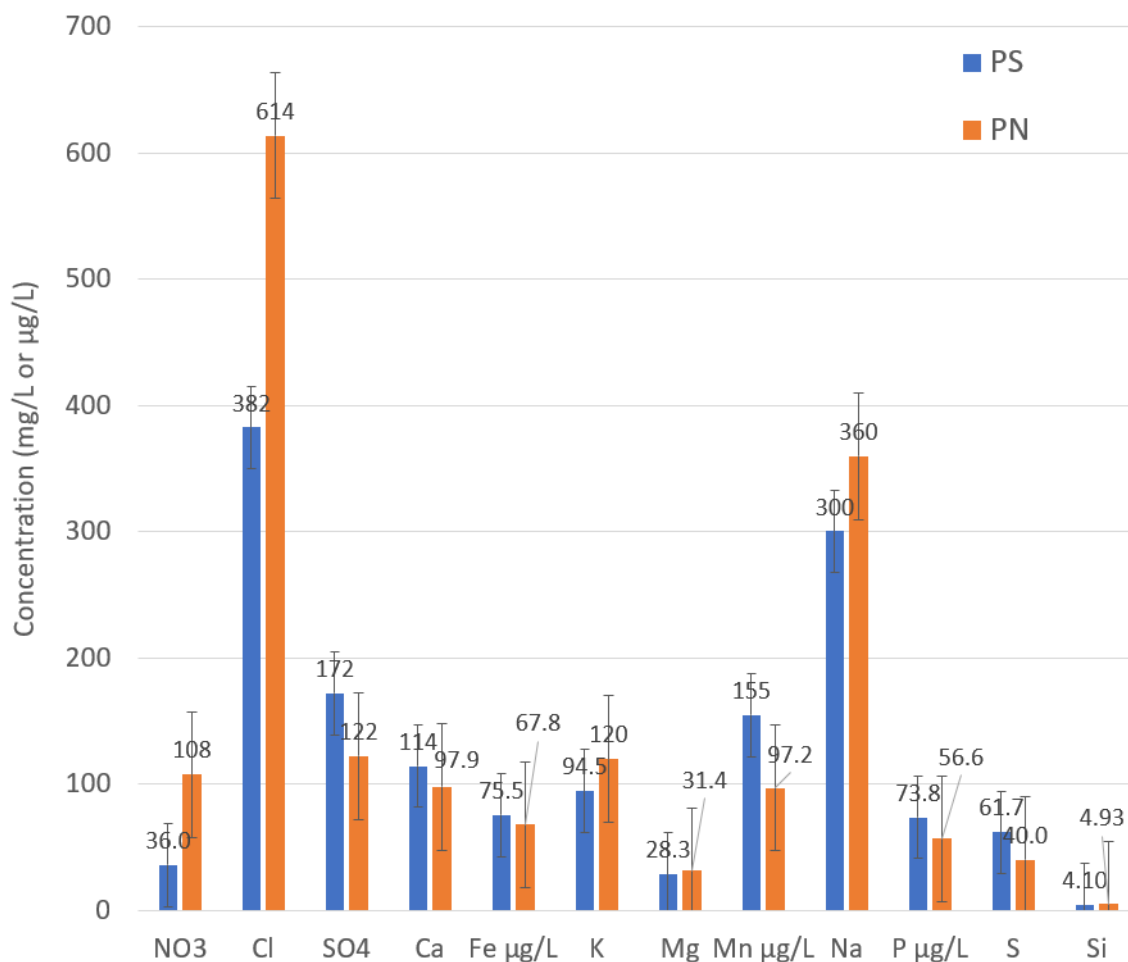


Figure 13: Mean concentration for macro ions in the polishing ponds (2021-2022) with standard error bars. Note the different unit for manganese, iron and phosphorus.

It is of interest to see if there is a difference between the polishing ponds, to help the process of tracing the source of the unknown inflow. The concentration of heavy metals are higher in PN for 11 out of 15 elements (Fig. 14 and 15).

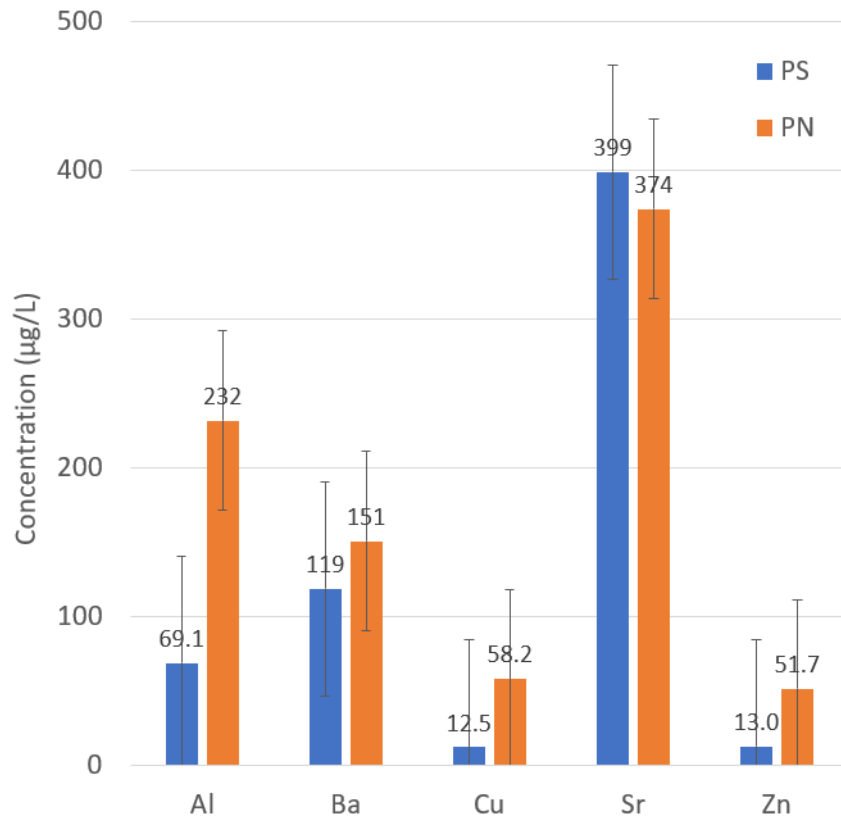


Figure 14: Mean concentration for some metals in the polishing ponds (2021-2022) with standard error bars.

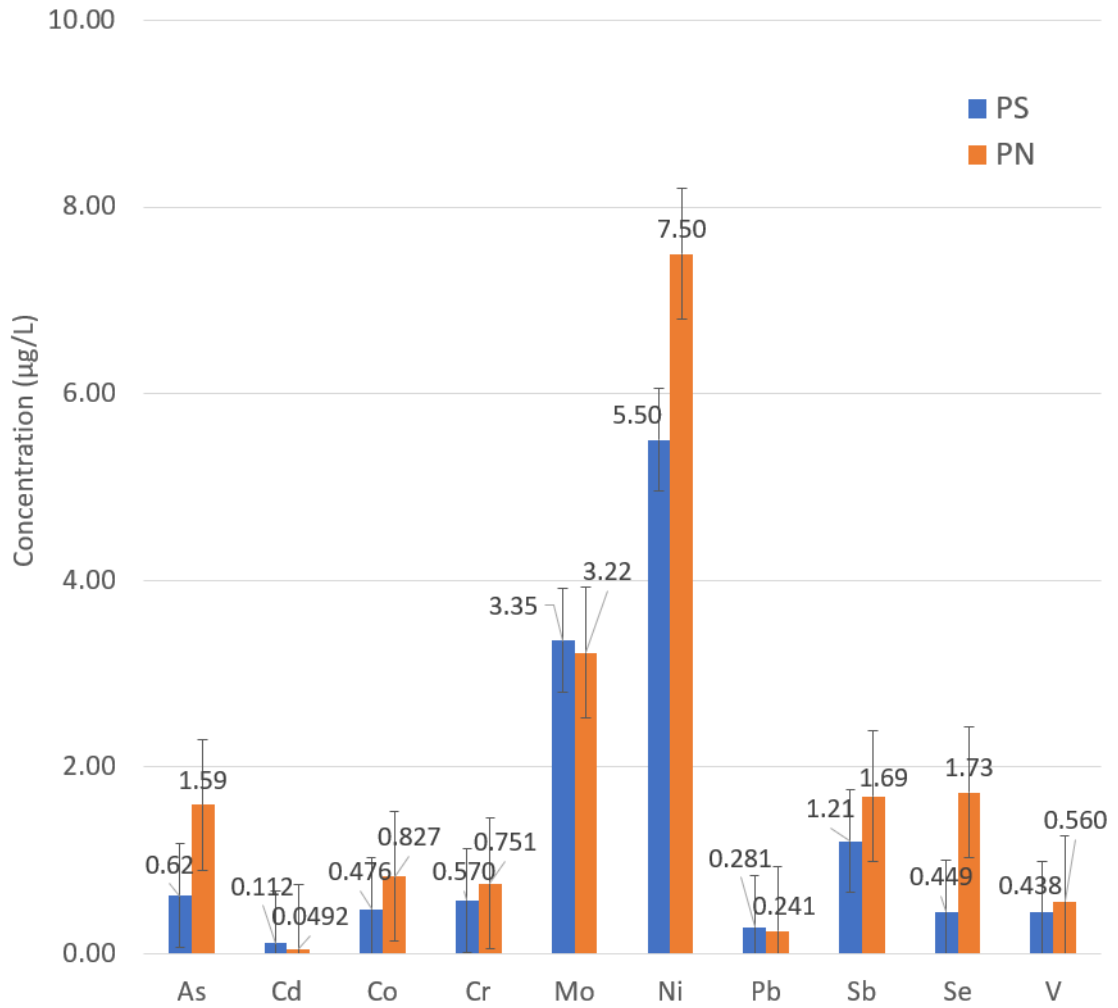


Figure 15: Mean concentration for some metals in the polishing ponds (2021-2022) with standard error bars.

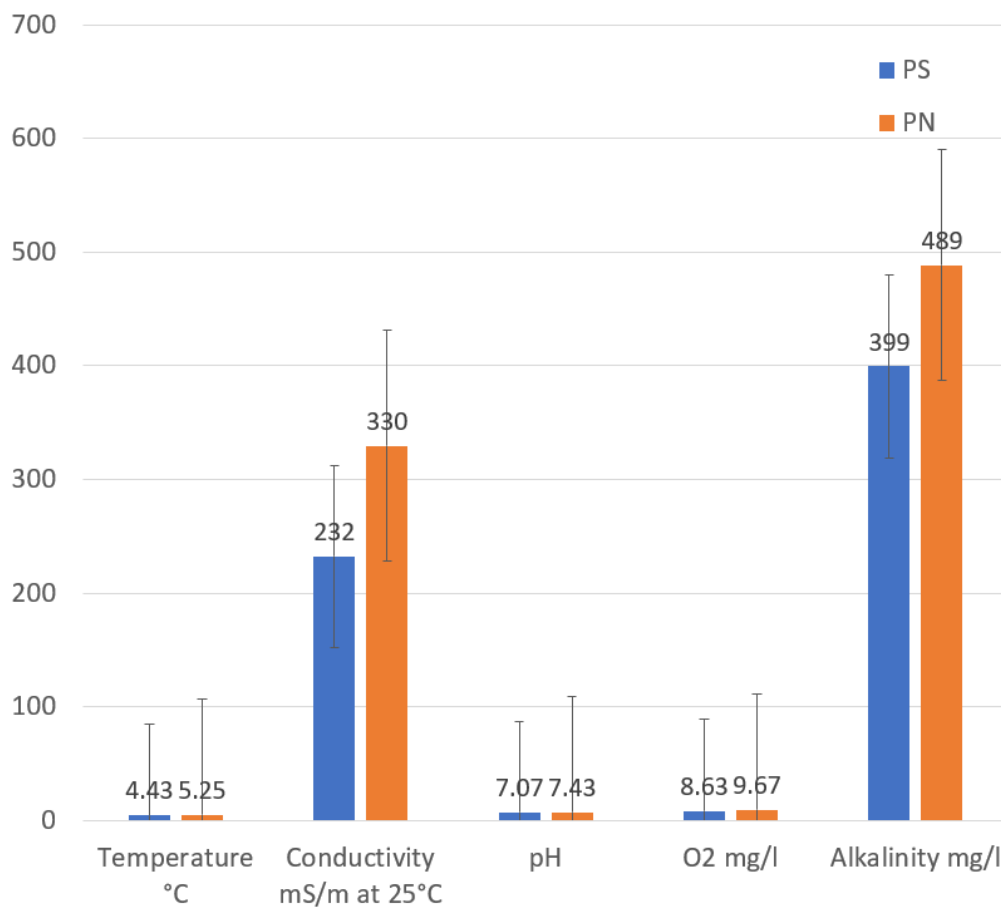


Figure 16: Mean concentration for some field parameters in the polishing ponds (2021-2022) with standard error bars.

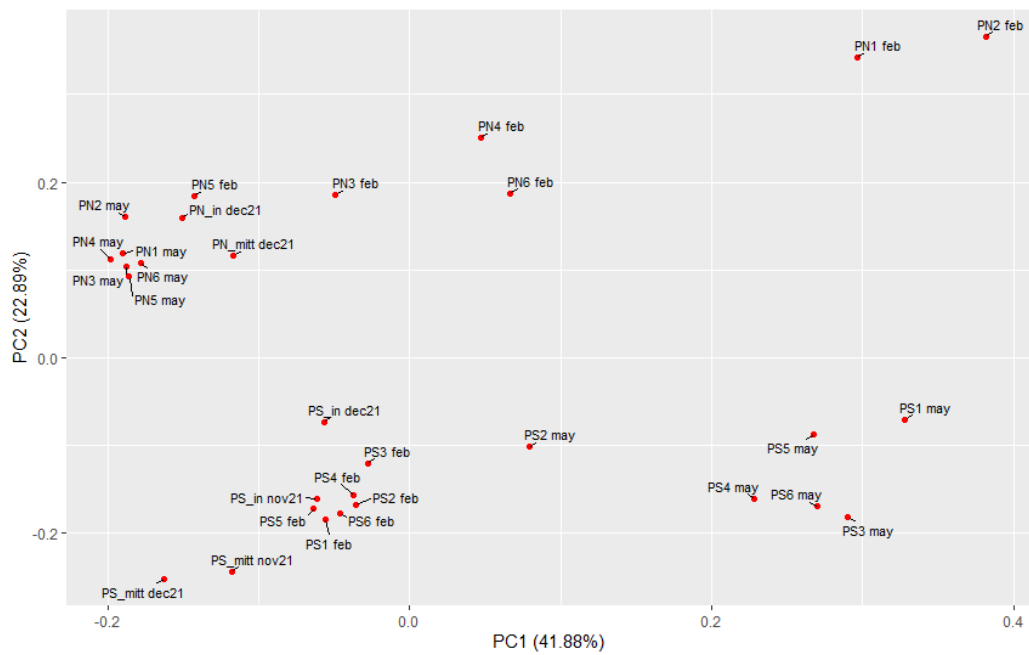
#### 4.1.4 Charge Balance

Since data was missing for some samples, the charge balance (Table 6) is incomplete for the groundwater samples. For the mean value for PN and PS, the charge balance is somewhat positive.

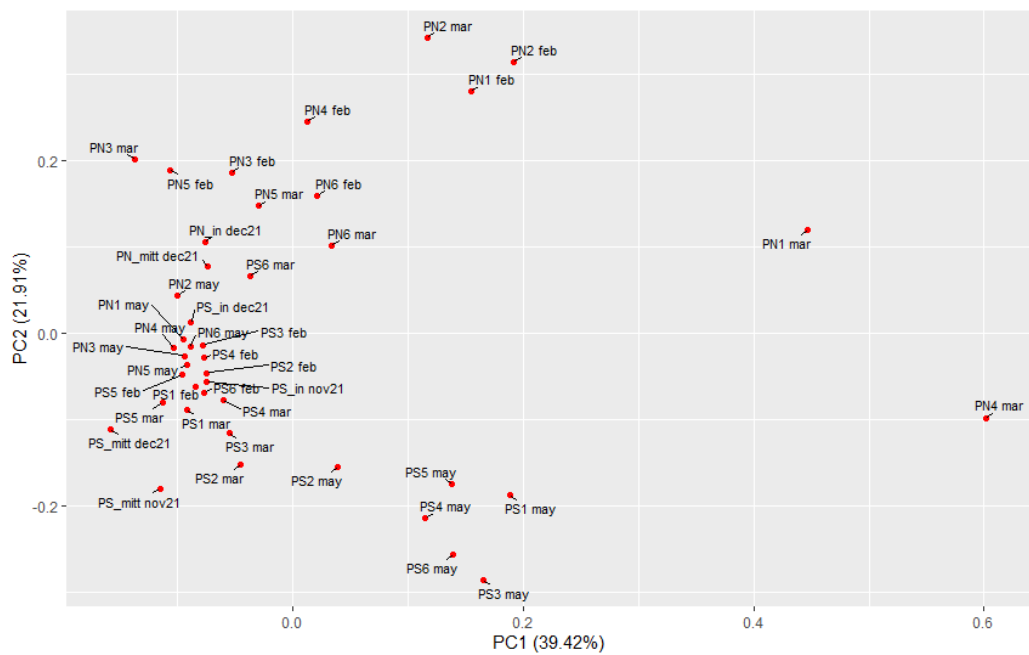
#### 4.1.5 PCA for polishing pond data

There is a clear difference in composition between PN and PS (Fig. 17a, 17b and 18). In 2021, fewer samples were taken in the ponds, but also these samples followed the same pattern. This difference was also indicated in Fig. 13-16, but less apparent. Due to lack of data in March, chloride and sulphate values were excluded from the analysis. In the resulting plot Fig. 17b, PS and PN are not as

distinctly separated as in Fig. 17a. Both Fig. 17a and Fig. 17b captures similar percentage of variance (65 % and 61 %, respectively). In PCA, points closer to each other are more similar than point further away from each other. There is a difference between samples taken in February and May (Fig. 17a), since these samples are generally separated in different clusters. This indicates a seasonal variation in both ponds. The effect seems to be opposite in PS and PN; for PS the samples have a higher value for PC1 in May than in February, while the opposite is true for PN. However, this is not as visible in Fig. 17b. In PN, the inflow samples (PN1 and PN2) were generally separated from the cluster. This is reasonable since most sedimentation is likely to happen there, since a turbidity curtain decreases the water flow speed which facilitate sedimentation. A corresponding pattern in PS is however not apparent, despite also having a turbidity curtain.



(a) All variables for nutrients and heavy metals



(b) Chloride and sulphate excluded.

Figure 17: PCA using nutrients and heavy metal data from 2021 and 2022 for the polishing ponds using log data.

Generally, ions such as sodium, magnesium and chloride are more important for the first component and metal ions, such as copper, aluminum and zinc, are more important for the second component. Ions that are more similar tends to be lumped together, as expected (Fig. 18). Iron stands out from the other macro ions, being negative correlated with them. Sulphur and sulphate appears to be associated with PS samples from November, December and February (Fig. 18).

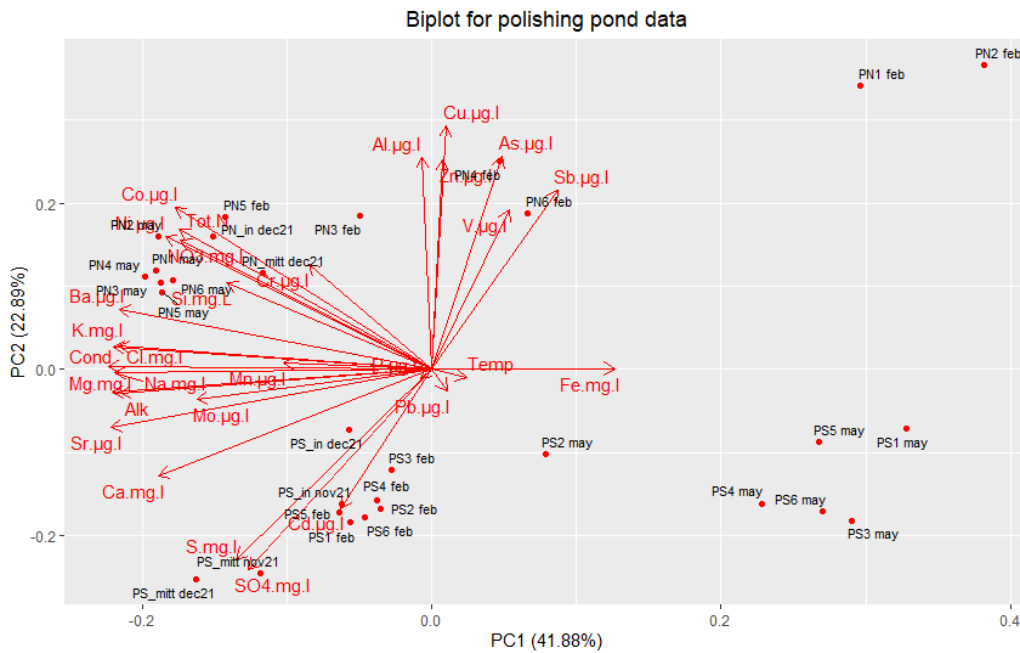


Figure 18: Biplot using nutrients and heavy metal data from 2021 and 2022 for the polishing ponds using log data.

## 4.2 Groundwater Analyses

### 4.2.1 Groundwater quality

Groundwater well data was summarised in Table 4.

Table 4: Groundwater data. The data includes all groundwater wells and samples found in Table 1. The number of samples for each variable is denoted n.

	<b>Unit</b>	<b>Mean</b>	<b>Median</b>	<b>Max</b>	<b>Min</b>	<b>n</b>
Temperature	°C	11.0	10.2	20.5	3.8	36
Conductivity	mS/m at 25°C	264	179	857	47.3	39
pH		6.98	7	9.4	6.1	43
O2	mg/L	3.28	3.4	5.72	1.25	29
Water level	cm	168	123	1140	0.83	40
Alkalinity	mg/L	452	341	1690	31.9	48
Ammonium	mg/L	5.56	0.292	99	0.01	48
NO3-	mg/L	66.3	4.02	600	ND	18
NO3- as nitrogen	mg/L	14.5	1	130	ND	19
NO2- as nitrogen	mg/L	0.204	0.023	4.2	0.0033	43
TotN	mg/L	13.5	1.96	120	0.15	40
Cl	mg/L	343	148	1460	5.7	37
SO4	mg/L	317	310	840	1.5	37
Al	µg/L	234	41.1	2840	0.1	49
As	µg/L	0.832	0.484	6.38	0.0805	49
Ba	µg/L	96.6	75.2	325	1.69	49
Ca	mg/L	198	197	452	2.96	49
Cd	µg/L	0.115	0.0495	0.7	0.001	49
Co	µg/L	0.926	0.743	4.09	0.0025	49
Cr	µg/L	0.618	0.374	3.19	0.005	49
Cu	µg/L	8.47	4.35	35.7	0.328	48
Fe	mg/L	1.50	0.0782	13.8	0.000483	49
Hg	µg/L	0.0262	0.0148	0.0922	0.00221	11
K	mg/L	50.3	11.8	254	1.02	49
Mg	mg/L	34.2	25.6	101	0.631	49
Mn	µg/L	750	297	4940	0.578	49
Mo	µg/L	2.31	2.12	8.16	0.058	49
Na	mg/L	216	104	935	5.18	49
Ni	µg/L	4.45	2.68	21.4	0.025	49
P	µg/L	88.7	21.4	848	0.5	49
Pb	µg/L	1.14	0.221	10.8	0.005	49
S	mg/L	101	96.8	254	0.295	49
Sb	µg/L	0.278	0.212	0.826	0.0168	49
Se	µg/L	25.1	1.375	284	0.325	26
Si	mg/L	7.82	7.97	13.4	0.399	49
Sr	µg/L	620	465	2110	33.2	49
V	µg/L	1.39	0.697	6.43	0.00579	49
Zn	µg/L	26.0	4.06	420	0.298	49

Analysis of groundwater data suggests that 18G09, P3 IN and P8 were mostly affected at the landfill. Water quality data indicates that these wells in general have higher macro ion concentration as well as higher conductivity and alkalinity. However, for total nitrogen, the concentrations were clearly the highest at sites P2 and P6, and for calcium, the concentrations were more similar but highest at sites P1, P2, P3 IN, P6 and P8. The sulphate concentrations were the highest at sites P3 IN, P1 and P2.

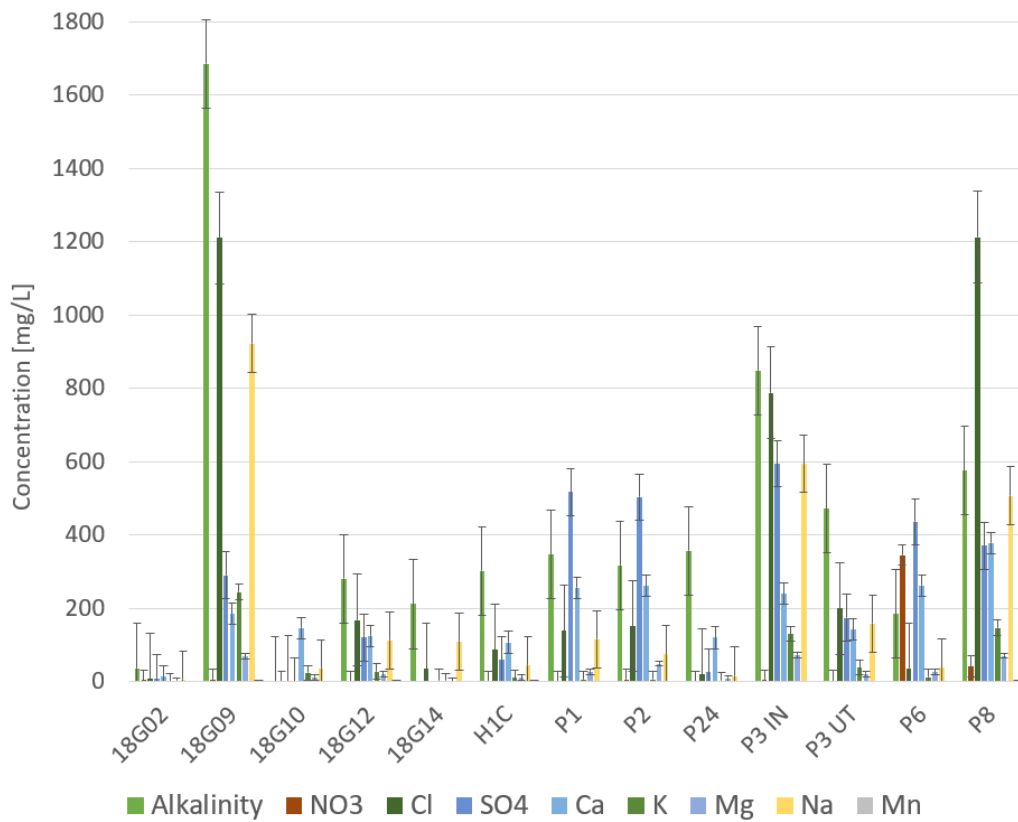


Figure 19: Mean of selected groundwater data parameters from 2021 and 2022 with standard error. For bars without standard error, only one sample was available. For 18G14, only one sample for all variables was available.

#### 4.2.2 PCA for groundwater data

In Fig. 20, the first principal component (Comp 1.) is likely to represent the magnitude of impact of the landfill on the wells. The further to the right, the less affected the well were by the landfill and vice versa. This is further indicated in the biplot (Fig. 21). This is well in line with the assumption that 18G02 is

unaffected (which is why it is used as a reference well). 18G14 is a deep bedrock well with another type of groundwater than the other wells, which can explain the data point's peripheral position in the plot. P24 is situated close to the west border of the landfill and also has a low magnitude of impact from the landfill, as seen in the plot. The wells P3 IN and P3 UT are spatially close, but since there is a barrier between them, P3 UT is much less contaminated, which is also shown in the plot. This is most clear when comparing samples from the same month, as expected. The first and second PC explains a total of 70% of the variance, 54% and 16% respectively.

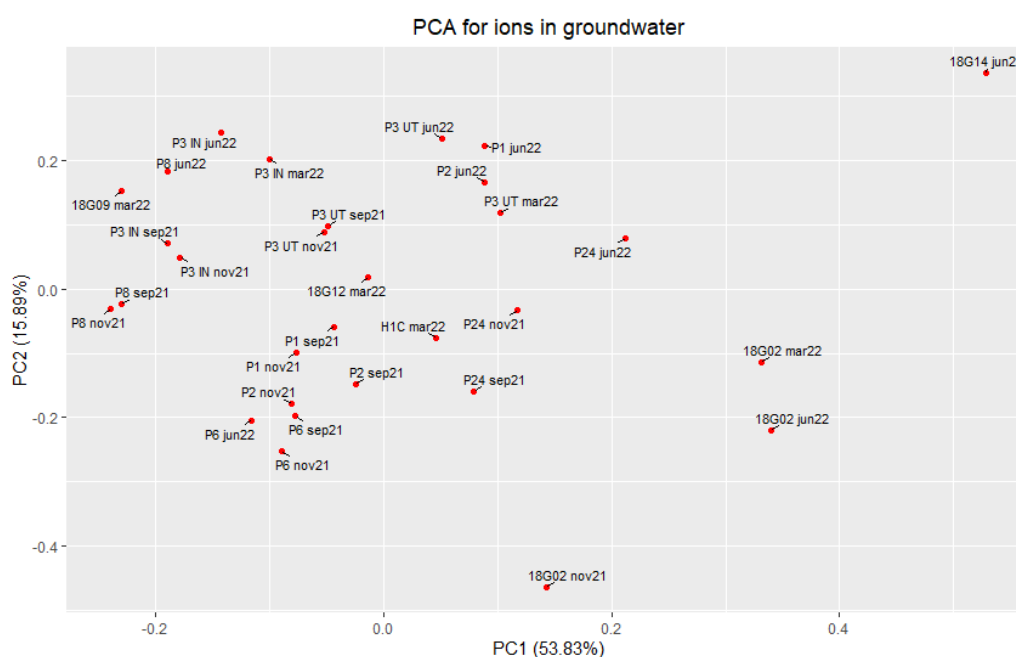


Figure 20: PCA using nutrients and heavy metal data from 2021 and 2022 for groundwater water using log data.

It would be expected for ammonium and total nitrogen (TotN) to be closely related, however this is not the case (Fig. 21). In general, the loading vectors for heavier metal ions are pointing in negative PC2 direction, while for macro ions, they are pointing in positive direction for PC2.

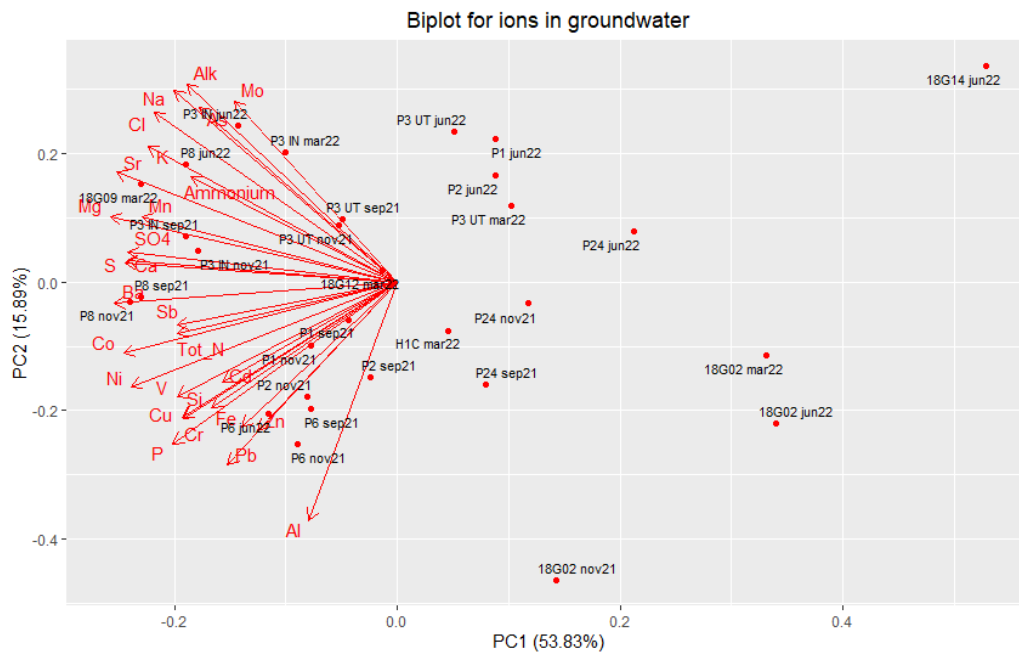


Figure 21: Biplot using nutrients and heavy metal data from 2021 and 2022 for groundwater using log data.

### 4.3 PFAS Analyses

The most commonly detected PFAS were PFOA, PFOS, PFBS, PFHxA and PFHpA, all detected in 90 % or more in the surface water and groundwater samples (n=23) (Fig. 22).

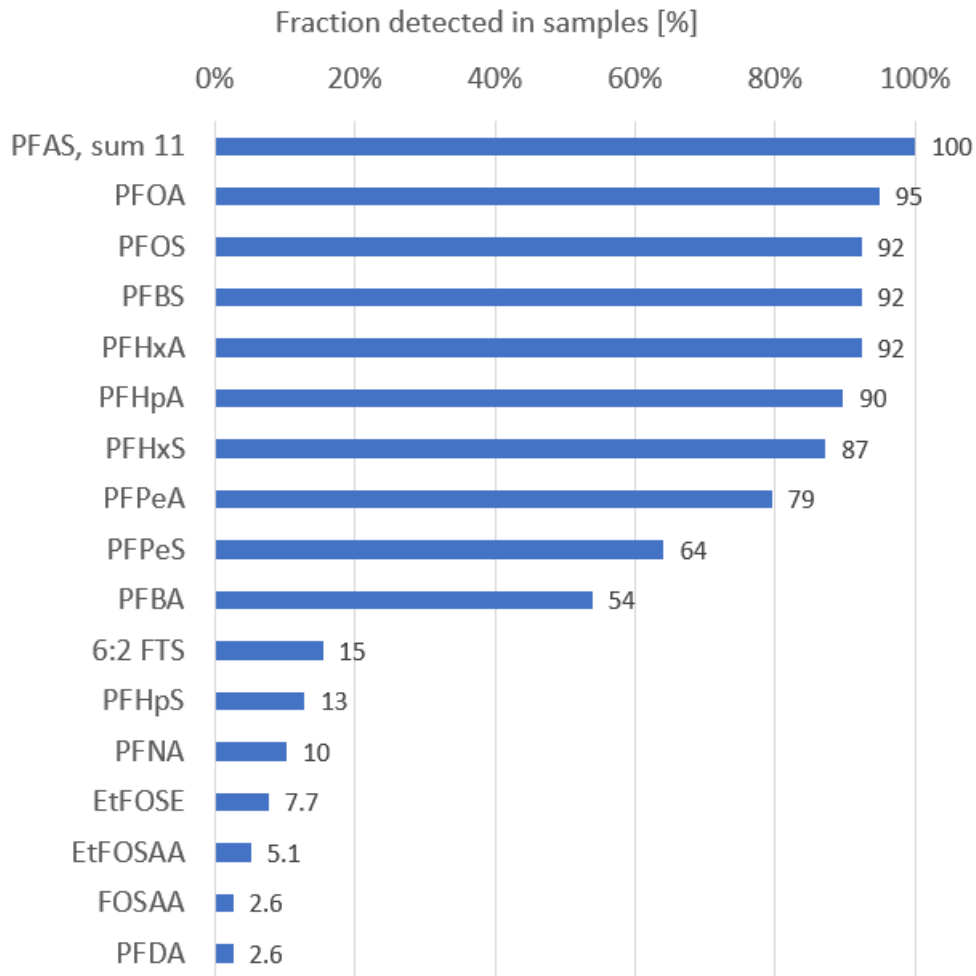


Figure 22: The fraction of PFAS detected in surface water and groundwater samples. Several other PFASs were included in the analysis, but since they were not detected, they are not included in the plot.

#### 4.3.1 Groundwater

The average  $\Sigma_{11}$ PFAS concentration was  $0.712 \mu\text{g/L}$ , while the median was  $0.379 \mu\text{g/L}$  (n=23). The highest concentration of PFAS was found in 18G09 (Fig. 23).

Also P3 IN nov shows a high total concentration of PFAS. For P3 IN and P3 UT, total concentration was higher in November 2021 than in March 2022 (Fig. 23). The sum PFAS concentration in 18G02 was very low both in November 2021 (0.00056  $\mu\text{g/L}$ ) and in March 2022 (0.00081  $\mu\text{g/L}$ ), as expected.

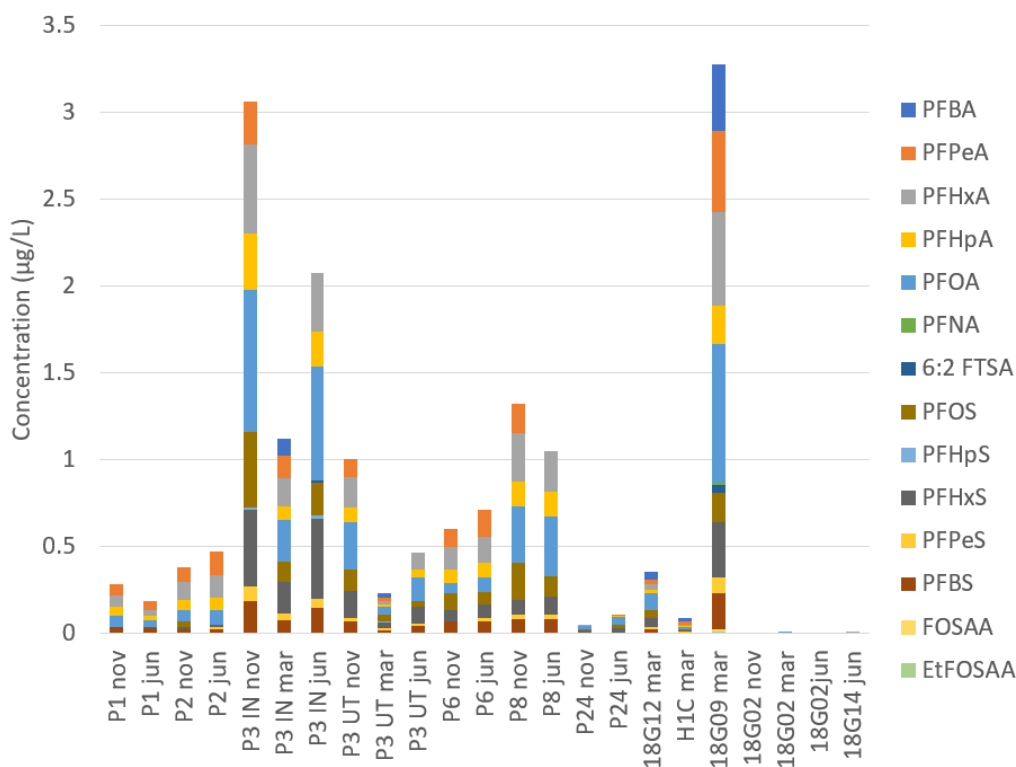


Figure 23: Sum PFAS concentrations in groundwater samples at Hovgården. Values under the detection limit were set to zero.

In general, C<sub>4</sub>-C<sub>8</sub> PFCA:s made up the largest fraction of PFASs in groundwater samples. This fraction made up the smallest part of all samples in P3 UT in the March 2022 sample. PFOA was the largest fraction in most groundwater samples (13 of a total of 23), followed by PFBA (5), PFPeA (4), and PFHxA (2). In P2, the PFBA and PFHxA fractions were equal (21%). The PFBA fraction was largest in the 18G02 samples (45%, 37% and 39%). The mean fraction of PFCAs (PFBA, PFPeA, PFHxA, PFHpA, PFOA, PFNA, PFDA) was 71% and the mean fraction of PFSA:s (PFBS, PFHxS, PFOS, PFPeS, PFHpS) was 28%.

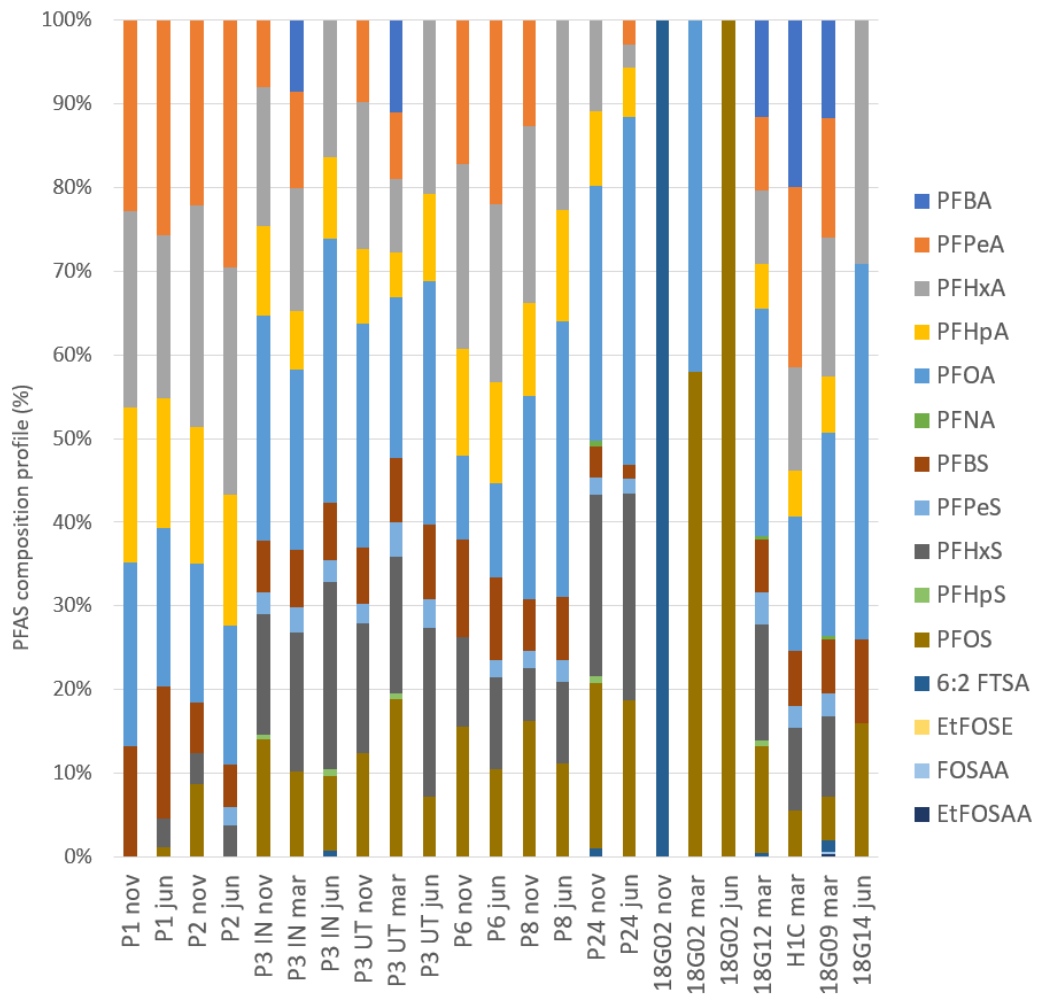


Figure 24: Fractional distribution of PFAS in groundwater in Hovgården. Values under the detection limit were set to zero.

The 18G02 well stands out and is clearly separated from the other wells (Fig. 25), which was expected since it is used as a reference well and is very little affected by the landfill. The first and second PC explains a total of 64% of the variance, 40% and 24% respectively.

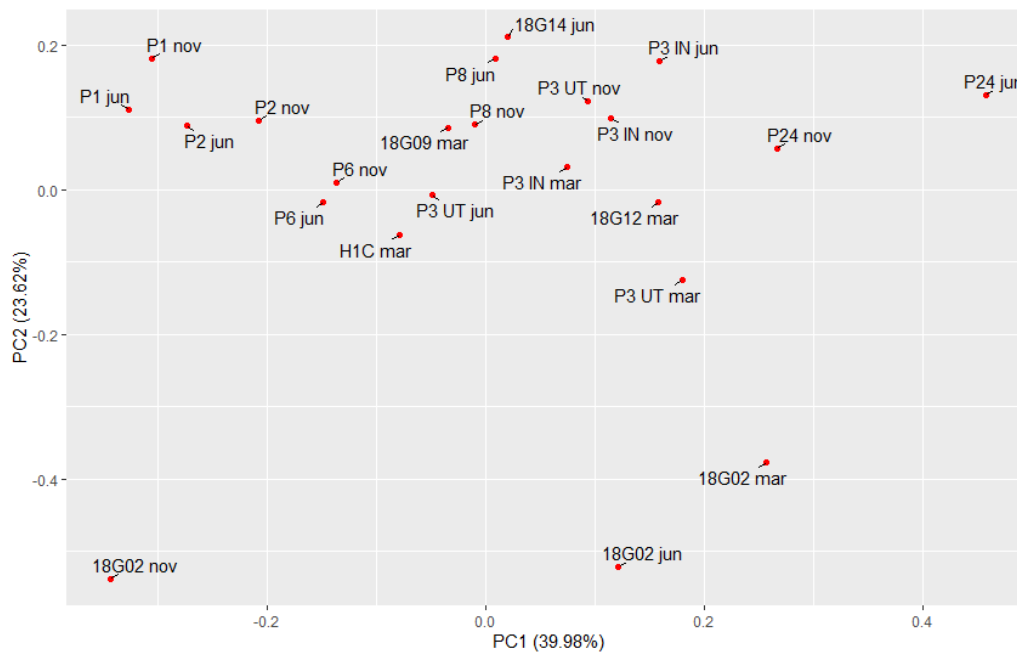


Figure 25: Results from the PCA analysis of PFAS composition (fingerprint) in groundwater. November (“nov”) samples were sampled in 2021 and March and June (“mar” and “jun”, respectively) were sampled in 2022.

The PFAS concentration in 18G02 was very low (Fig. 23) and it is quite separated from the other wells in the PCA (Fig. 25). Thus, a PCA analysis was performed without 18G02 (Fig. 26-27). The captured variation increases somewhat (70%). The 18G14 well now is now separated from the other wells, again likely due to the fact that it is another type of well. Samples from the same well, taken in different seasons, are generally close (Fig. 26).

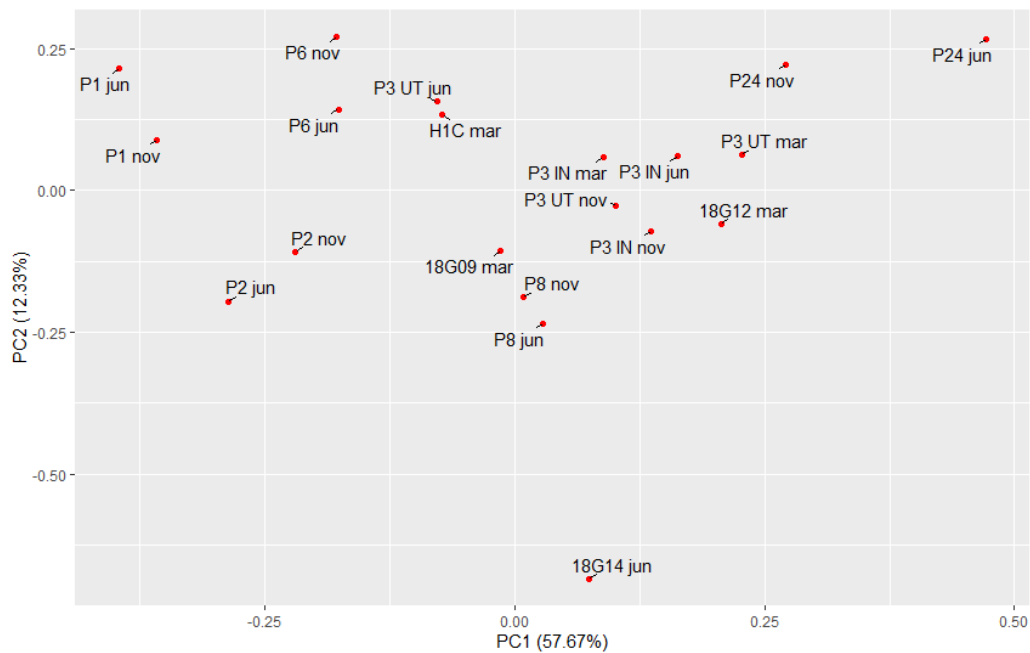


Figure 26: Results from the PCA analysis of PFAS fingerprint in groundwater. Three samples from 18G02 was excluded in this analysis. November ("nov") samples were sampled in 2021 and March and June ("mar" and "jun", respectively) were sampled in 2022.

Generally the loading vectors are quite long and so the biplot seems to capture a lot of the variability of the data. PFOS, PFBS and PFPeA appears to be important for PC1, while for PC2, PFPeS and PFHxA are important.

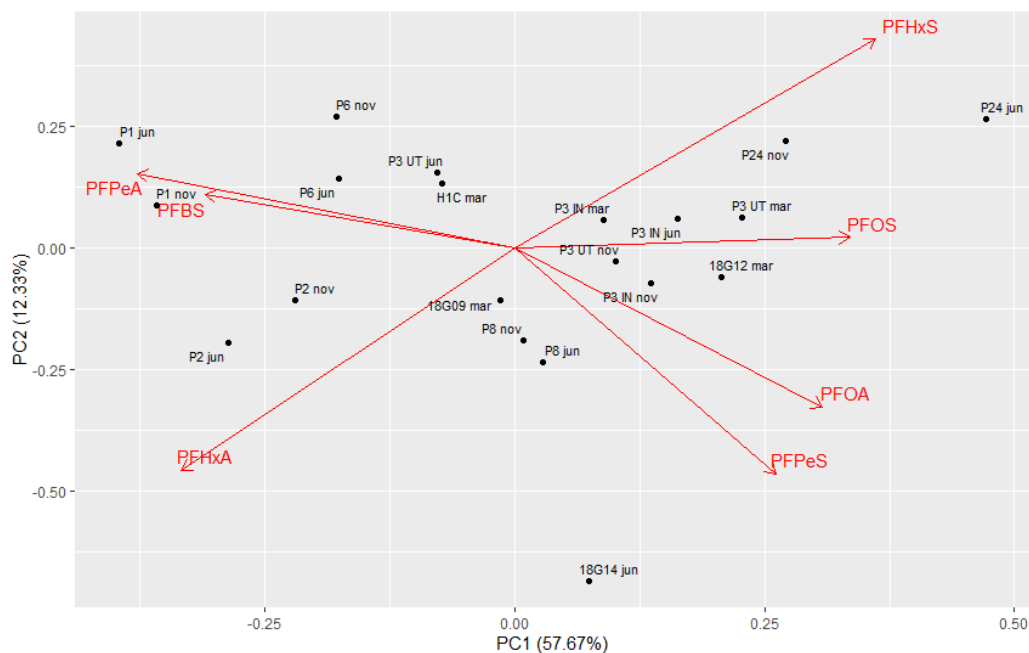


Figure 27: Results from the PCA analysis of the PFAS composition (fingerprint) in groundwater. Three samples from 18G02 was excluded in this analysis. November ("nov") samples were sampled in 2021 and March and June ("mar" and "jun", respectively) were sampled in 2022.

#### 4.3.2 Ponds and WWTP water

The average PFAS $\Sigma_{11}$  concentration was 0.665  $\mu\text{g/L}$ , while the median was 0.633  $\mu\text{g/L}$  (n=16). The highest  $\Sigma\text{PFAS}$  concentration was found in the inlet to the wastewater treatment plant, R1 (1.75  $\mu\text{g/L}$ ). The  $\Sigma\text{PFAS}$  concentration then decreased when measured in R3 and R4, being lower in R4. In the outlet from the sedimentation pond, the concentration was higher than in R4 but lower than in R3. This could be due to water from R3 and R4 being mixed again. The concentration in the south polishing pond is fairly consistent, while in the northern pond PN1, PN2 and PN4 are notably lower (Fig. 28).

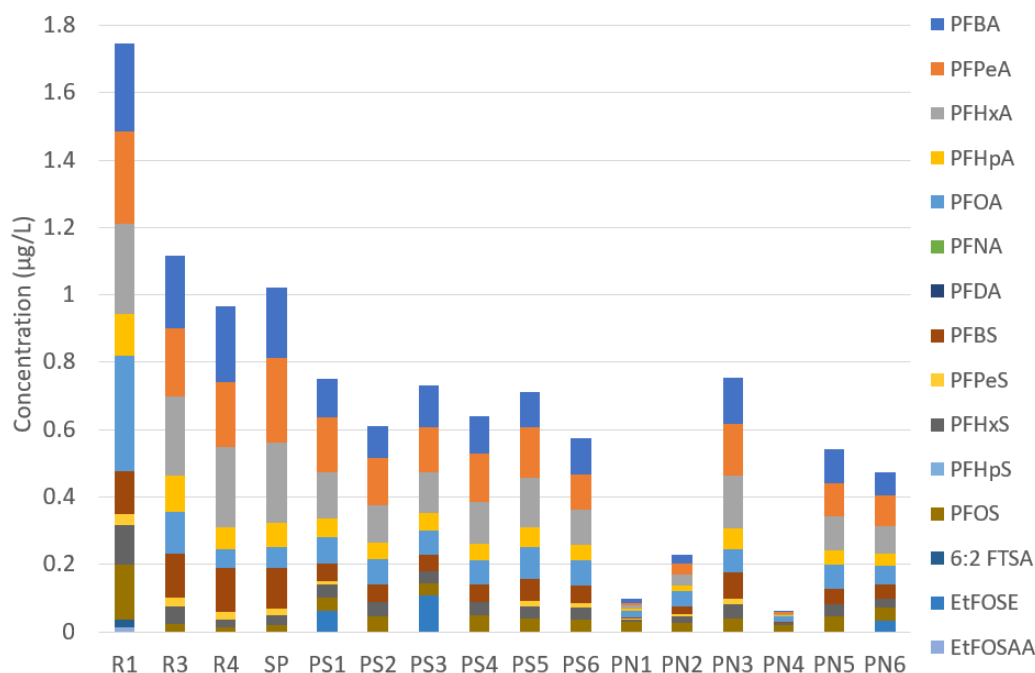


Figure 28: Concentration of PFAS in the WWTP and surface water in Hovgårdén. Samples under the detection limit was set to zero.

### *PFAS Fingerprinting*

PFPeA had the highest fraction in most of the surface water samples (9 of a total of 9), followed by PFHxA and PFOA (4 each). Some samples had the same fraction for two PFASs. The distribution of PFAS in the surface waters appears to be somewhat similar, with some exceptions. EtFOSE was detected in PS1, PS3 and PN6 (Fig. 29) while not being detected in any of the WWTP samples (Fig. 29), or any of the groundwater samples (Fig. 24). The mean composition of PFCAs (PFBA, PFPeA, PFHxA, PFHpA, PFOA, PFNA, PFDA) were higher in PS (75%) than in PN (66%), and the mean composition of PFSAs (PFBS, PFHxS, PFOS, PFPeS, PFHpS) are higher in PN (33%) than in PS (21%). The mean fraction in all surface water samples were 72% for PFCAs and 26% for PFSAs. There is a large fraction of PFOS in PN1 and PN4. PN4 was the only sample where PFDA was detected, however in very low concentration (0.00053 µg/L).

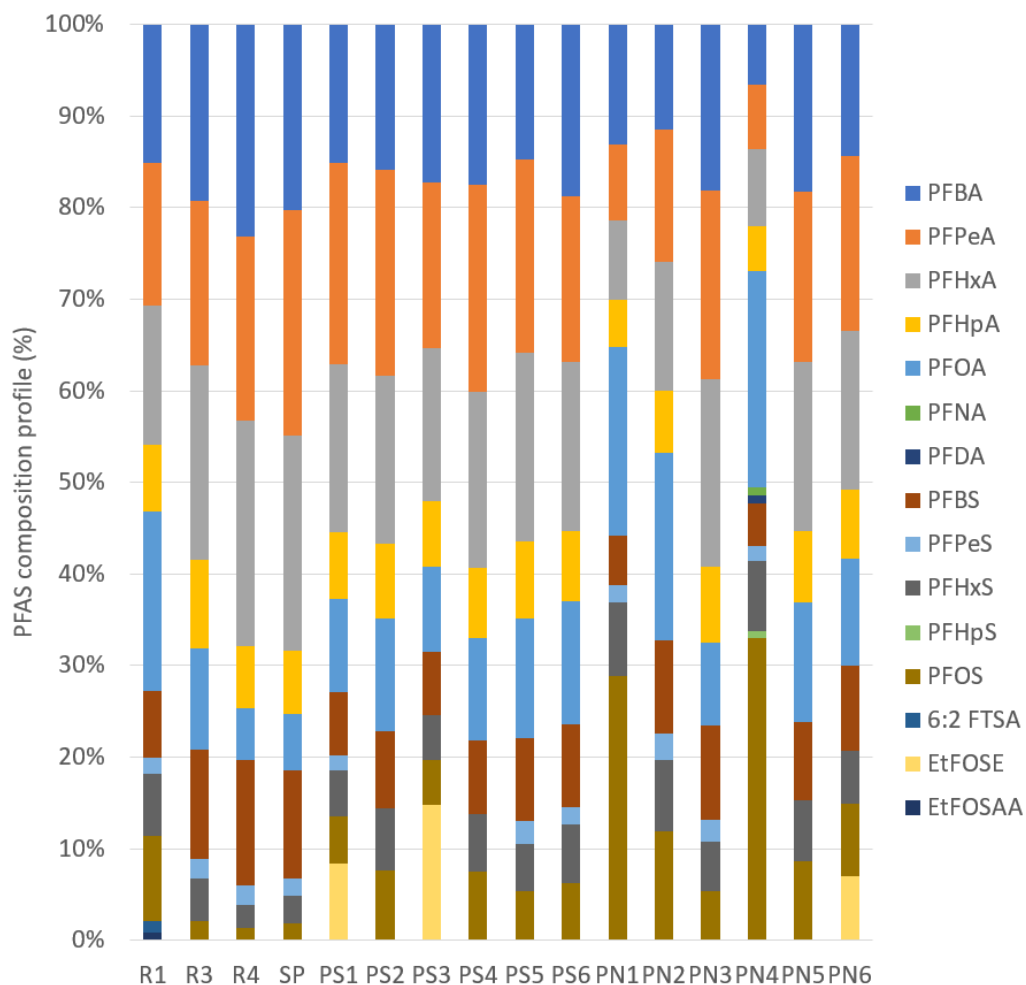


Figure 29: PFAS composition profile in the WWTP and surface water in Hovgården. Samples under the detection limit were set to zero.

In Fig. 30, there appears to be two or three groups. PN1 and PN4 are situated separated of the other samples in surface water. R1 and PN2, though closer to the rest of the sample points, are also quite separate. The first and second PC explains a total of 83% of the variance, 69% and 14% respectively.

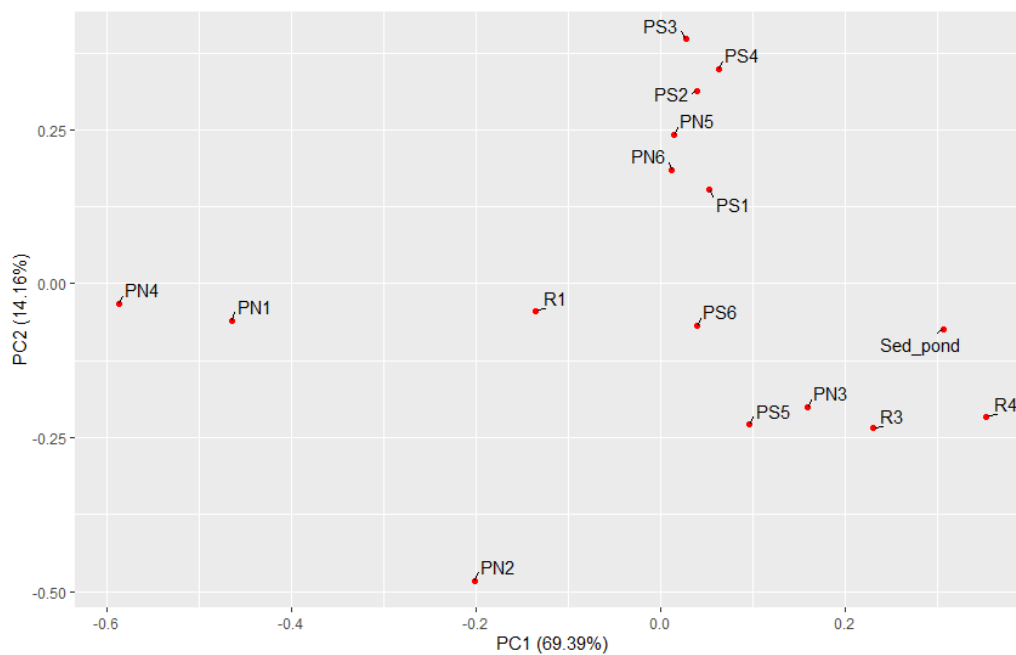


Figure 30: Results from the PCA analysis of the PFAS composition (fingerprint) in surface water. All sampling points were sampled in March 2022 (Table 1). Sedpond is the sedimentation pond.

PFPeS is clearly important for PC2, while the other PFASs contribute to PC1. The PFASs with longer chains (PFOS, PFOA and PFHxS) point towards R1 and are negatively correlated with shorter-chained PFASs (Fig. 31). It is reasonable that longer-chained PFASs are found in the beginning of the wastewater treatment.

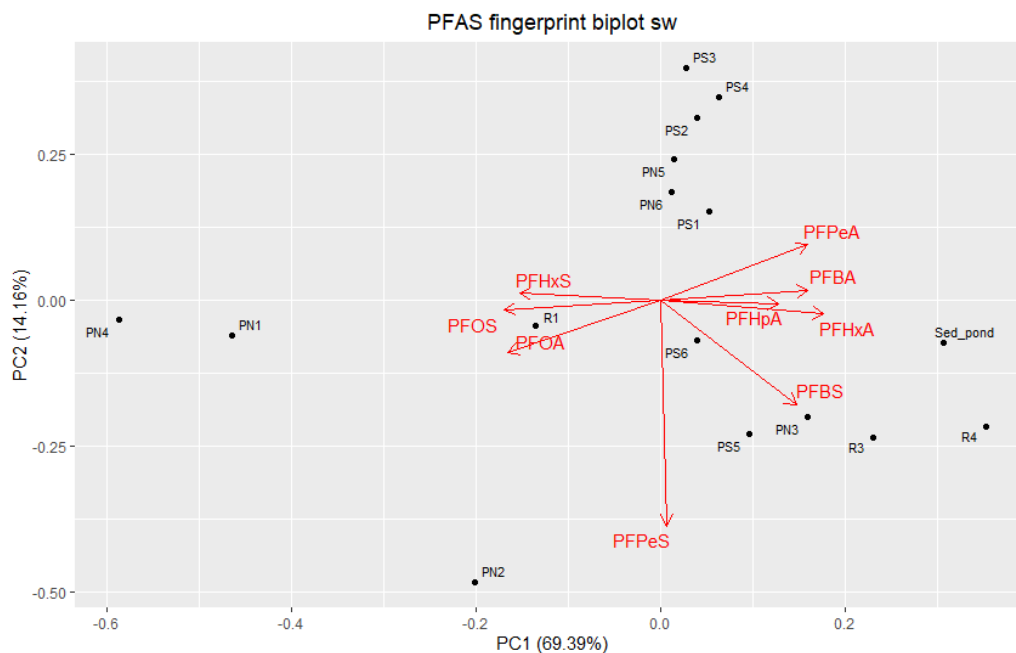


Figure 31: Biplot of the PCA analysis of the PFAS composition (fingerprint) in surface water. All sampling points were sampled in March 2022 (Table 1). Sedpond is the sedimentation pond.

### 4.3.3 Correlation analysis

The strongest correlation between the PFAS compositions were found for PFOA: a negative correlation with PFPeA ( $r=-0.72$ ,  $p=2.6E-07$ ), a positive correlation with PFHxS ( $r=0.70$ ,  $p=8.8E-07$ ) and a negative correlation with PFBA ( $r=-0.65$ ,  $p=9.2E-06$ ). Also PFOS had a clear negative correlation with PFPeA ( $r=-0.69$ ,  $p=9.7E-07$ ) and PFBS had a clear positive correlation with PFHxA ( $r=0.66$ ,  $p=5.6E-06$ ). All these correlations were statistically significant (Table 5).

Table 5: Pearson correlation analysis of PFAS composition (fingerprint) data for groundwater and surface water. Only PFASs with values for all samples were included. Samples under the detection limit was divided by two if the number of detected samples for a variable exceeded 50%. 18G02 was included in the data set.

		PFBA	PFPeA	PFHxA	PFHpA	PFOA	PFBS	PFHxS	PFOS	PFPeS
PFBA	r-value	1	0.34	-0.19	-0.31	-0.65	-0.11	-0.59	-0.24	0.33
	p-value		0.033	0.25	0.055	9.20E-06	0.49	7.5E-05	0.15	0.042
PFPeA	r-value		1	0.30	0.093	-0.72	0.28	-0.56	-0.69	-0.42
	p-value			0.062	0.57	2.6E-07	0.080	0.00022	9.7E-07	0.0086
PFHxA	r-value			1	0.59	-0.32	0.66	-0.45	-0.58	-0.43
	p-value				9.0E-05	0.051	5.6E-06	0.0044	0.0001	0.0069
PFHpA	r-value				1	-0.065	0.40	-0.17	-0.36	-0.42
	p-value					0.70	0.012	0.29	0.024	0.0085
PFOA	r-value					1	-0.40	0.70	0.46	0.11
	p-value						0.013	8.8E-07	0.0036	0.51
PFBS	r-value						1	-0.39	-0.43	-0.17
	p-value							0.014	0.0065	0.30
PFHxS	r-value							1	0.43	0.20
	p-value								0.0064	0.23
PFOS	r-value								1	0.27
	p-value									0.10
PFPeS	r-value									1
	p-value									

#### 4.3.4 PCA for PFAS in surface water and groundwater samples

The first and second PC explains a total of 69% of the variance, 55% and 14% respectively (Fig. 32) for PFAS in surface water and groundwater samples. There are no clear grouping of the data points, and data points of the same type (groundwater or surface water) are closer together. The data points PN1 and PN4 sampled in March are separated from the rest of the surface water samples. The June samples from two wells (P24 and P1) are somewhat peripheral to the main data cluster. This might be due to their relatively small fraction of PFBA (between 2-6%), compared to the groundwater sample mean (16%) and median (12%). The fraction of PFBA in groundwater was lower in June than in November and March for all samples except for 18G02.

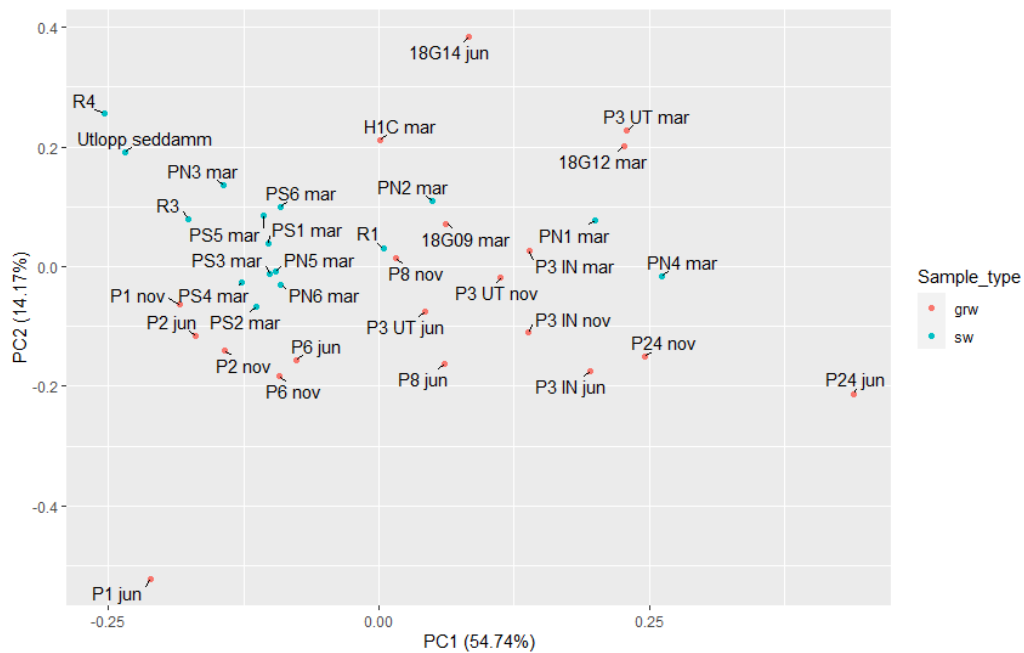


Figure 32: PCA of PFAS composition (fingerprint) for groundwater (red dots) and surface water (blue dots) at Hovgården. The well 18G02 was excluded from the analysis.

PFBA, PFPeS and PFHpA influence PC2, while the other PFASs are associated with PC1. PFBA, PFBS and PFHxA appears to be more associated with the WWTP and ponds, while in general PFASs with longer chains (PFOA and PFOS) appears to be more associated with groundwater (Fig. 33).

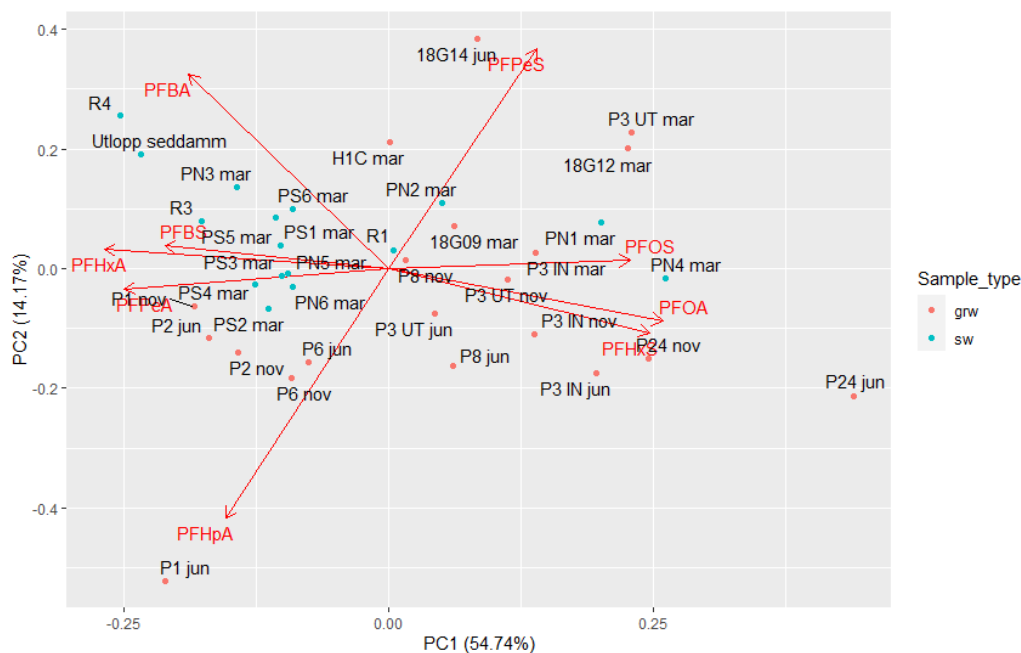


Figure 33: Biplot of PFAS composition (fingerprint) for groundwater (red dots) and surface water (blue dots) at Hovgården. The well 18G02 was excluded from the analysis. Utlopp seddamm is the sedimentation pond sample, taken by the outlet.

## 5 Discussion

### 5.1 Transport of ions and PFASs to the ponds

#### *Mass Flow*

The mass balance shows that there is an evident additional flow of contaminants to the ponds (PS1-PS6, PN1-PN6), both of metals, nutrients (Fig. 2) and PFASs (Fig. 10). The calculated concentration in the unknown flow (Table 3) is in the same order of magnitude as is the inflow to and outflow from the ponds as well as groundwater data (Table 4), which further strengthens the calculations. Had the concentrations been many orders of magnitude greater, it might indicate that the calculations are wrong. There was also a significant flow of heavy metal ions and other ions into the ponds (Table 2) from an unknown source. However, the addition of  $\Sigma_{11}$ PFAS to the polishing ponds must be regarded with caution, since it might be the degradation of PFAS precursors that is responsible for the increase in the sum of PFAS. There are thousands of PFASs, and only a handful are included in the analysis. Furthermore, PFAS precursors are not included in

$\Sigma_{11}$ PFAS. Nonetheless, considering the demonstrated inflow of ions, it is likely that there is also an inflow of PFAS. Worth emphasising is that the unknown flow might be more than one flow, and so the concentration in Table 3 is a mean concentration of these potential flows, which can have both higher and lower individual concentrations, stem from different sources and enter the ponds in different locations. This, naturally, complicates the task of tracing the water. Future analyses would benefit from performing a mass balance for each pond, which might further elucidate the unknown groundwater flow(s) to each pond.

#### *Water Distribution*

As an outcome of results presented in this study, a trace chemical color detection experiment was performed by Hovgården employees, which showed that the incoming water distributed differently in both ponds, with more water coming into PN compared to PS. The concentrations of water were similar when flowing into both ponds, however the concentration in PN might be affected by the higher water flow, since i) more particles can sediment, ii) chemicals can interact more with the water phase, iii) the samples were taken on different water for PS and PN, since the different water flows give the ponds different retention times. Depending on the conditions in the pond, chemicals can interact with the sediment (sorption and desorption processes), which can affect the concentration. The landfill leachate composition can vary greatly even in short time, and so if the water in the ponds differ in age, there is likely that their compositions are different as well. To determine this possibility, sediment in both ponds should be sampled in the future to see if there are any significant differences.

A difference in water flow distribution into the ponds might explain the differences between them. The lower flow through PS provides more time for particles to settle down and allows them to sediment, as well as for biological processes to occur. This could be the reason for the, in general, lower concentrations in PS. The differences in pH, temperature and oxygen between the ponds (Fig. 16) are probably too low to have an impact on the solubility of heavy metals. Biological processes in the ponds will however not affect PFAS since they are very recalcitrant substances, resistant to degradation.

#### *Differences Between the Ponds*

The PCA of metals and nutrients, including chloride and sulphate, shows a clear difference between the northern and southern polishing ponds (Fig. 17a). When chloride and sulphate data was excluded from the analysis, samples from PN and PS became closer together (Fig. 17b) (note the different scale in PC1 in Fig. 17a and 17b). The biplot (Fig. 18) shows that the first PC is mostly influenced by macro ions (such as calcium, potassium, chloride etc.) while the second PC is mostly influenced by heavy metals (such as copper, arsenic and zinc). A notable

difference is that the exclusion of chloride and sulphate enabled the inclusion of the March samples, which contributes to the appearance of a more compactly distributed plot in Fig. 17b. Nonetheless, either chloride or sulphate, or both, appears to have a distinct impact on pond data distribution, and that this impact seems to affect the PC2 the most. In the biplot it is visible that both sulphur and sulphate are important for PS (Fig. 18).

Interestingly, the loading vectors for aluminum and chloride are almost perpendicular, indicating no correlation (Fig. 18). This is unexpected, since aluminum and chloride are added together as a flocculating agent.

Another explanation to the difference between the ponds are that an unknown inflow is entering the southern pond. It has been reported by Hovgården that the ice in the southern pond melts faster than PN, despite a smaller inflow of warmer water from the WWTP and that it is more shadowy situated. If water from an unknown inflow is entering the ponds, the pond water could be diluted and the concentration of chemicals would decrease (Fig. 13-15). Another possibility is that the two ponds are connected at the ground separating the two ponds. Furthermore, the difference between the ponds could perhaps be due to the difference in vegetation in the ponds (which can be a result of the different lighting situations). However, most of the samples were taken before the vegetation season. From Fig. 18, neither of the two loading vectors representing nitrogen (TotN and  $\text{NO}_3$ ) indicate that nitrogen, a significant factor in restricting algal growth in lakes (Yaqoob et al. 2021), contributed to any of the principle components. Yaqoob et al. (ibid.) concluded that there are clear differences between open waters and waters covered by vegetation, in terms of physical and chemical composition. Further analyses are needed to determine the role of vegetation for the differences in pond water composition.

The PN1, PN2 and PN4 samples were very different from the other PN samples, and also different from the PS and WWTP samples (Fig. 28). A possible explanation to this is that something went wrong during the sampling or analysis of the samples. However, PN1, PN2 and PN4 from the February sampling stands out as well from the other pond samples (Fig. 17a), as does the March samples in Fig. 17b. Therefore, sampling and analysis error is then perhaps not the only explanation. The difference could also be due to the sampling conditions, however according to the field notes all samples from the northern pond were taken in the same way in both sampling occasions. It would be a good idea to retake these PN samples to see if the low PFAS concentrations are consistent. It is also unclear what effect the ice cover on the ponds has on the sample concentration. There is also a possibility that water is leaking from the pipe leading wastewater along the northern part of PN to the WWTP. The sampling points PN2, PN4 and PN6 are

closest to the pipe, and since PN2 and PN4 stands out from other samples, this could be a possible explanation.

## 5.2 Correlation between surface water and groundwater

### *PFAS*

Overall, the most detected PFASs in this study was PFOA, which was detected in 95% of all samples, followed by PFOS, PFBS and PFHxA (all 92%) (Fig. 22). The mean fraction of PFCAs and PFSAs were quite similar in surface water (72 % and 26 %, respectively) and groundwater (71% and 28%, respectively), in contrast to the results by Gobelius et al. (2018) where in groundwater the difference was much smaller. However, for surface water the fractions of PFCAs and PFSAs are very similar to those in Gobelius et al. (ibid.). The fact that the composition in groundwater and surface water is the same is quite surprising, since PFCAs in general move faster in soil than does PFSAs (ibid.). However, the distances the groundwater moves on Hovgården might be too short to result in any great changes in composition.

The data points of the same type (groundwater or surface water) in the PCA plot are normally closer together (Fig. 32). This is expected, since PFASs mobility is different in soil/groundwater and water and depends on chain length and PFAS type (ibid.).

The correlations between PFASs are often significant (Table 5). PFOA had some of the strongest correlations, especially the negative correlation to PFPeA and PFBA, but also to a strong positive correlation to PFHxS.

The total PFAS concentration entering the WWTP in R1 was quite high (1.75  $\mu\text{g/L}$ ), only the concentration of P3 IN (3.4  $\mu\text{g/L}$  in November 2021 and 2.3  $\mu\text{g/L}$  in June 2022) and 18G09 (3.3  $\mu\text{g/L}$ ) were higher. There might be a degradation of PFAS precursors, such as EtFOSAA (detected in R1 and 18G09) and FOSAA (detected in 18G09) that contributes to the high concentration in the WWTP.

EtFOSE, second highest in the degradation chain (after POSF), was measured in some of the polishing pond samples, but not in any of the WWTP (R1, R3 and R4) (Fig. 29) or the well samples (Fig. 24). This could be due to the EtFOSE concentration falling just under the detection limit, but the concentration of EtFOSE in PS3 was quite high (0.108  $\mu\text{g/L}$ ) and not close to the detection limit (the highest was 0.025  $\mu\text{g/L}$ ). There might also be an inflow from an unknown groundwater source, since it was not detected in any of the sampled wells. There might be some leaching from the sorting area (situated approximately 200 m south of P3 INSIDA (Fig. 5), since EtFOSE has been used in paper and packaging products.

The groundwater wells were sampled at different occasions. The detection limit might also explain why EtFOSE was detected in low concentrations in the ponds, but not in any of the wells. Since the water in the ponds has been treated it is clearer, which can give lower detection limits compared to more turbid waters.

### *Copper*

In the calculated difference between R34 and A1 (Table 3), the copper "concentration" from an unknown inflow is quite large (35.7  $\mu\text{g/l}$ ) compared to groundwater data (Table 4), where mean copper concentration was 8.47  $\mu\text{g/L}$  and the median 4.35  $\mu\text{g/L}$ . The highest concentration in groundwater is however close, which was found in P6. In general, the highest copper values were found in P6, P8 and 18G09.

## **6 Conclusion**

In this study, various ions, metals and PFAS have been investigated at the landfill site Hovgården in Uppsala to investigate how the different water flows contribute to the water quality of the polishing ponds.

The results suggest that there is an unknown additional flow of water and mass to the polishing ponds, resulting in elevated concentrations in the ponds comparing inflow and outflow data. The concentrations for ions, metals and  $\Sigma_{11}$ PFAS increased by 191-327%, 158-1577 % and 244 %, respectively. All tested ions increased, except chromium, iron and manganese. The concentration of ions in the ponds indicated that there is a difference between the ponds, which was further supported by the PCA analysis.

Highest concentrations of macro ions and PFAS were found in the groundwater wells P3 IN, 18G09 and P8, suggesting continuous monitoring in these wells and establishment of treatment options for removal of contaminants.

PCA has shown to be a suitable tool to show similarities and dissimilarities between samples. PFAS fingerprinting helped reduce dimensionality of data and showed interesting correlations between groundwater wells and the polishing ponds, respectively.

The difficulty in this study was to show a correlation between the ponds and groundwater, to determine where the unknown inflow derives. While no obvious source could be seen, this study presents some suggestions that might help further work tracing the water. Modelling approaches (e.g. hydrology modelling) are needed to further evaluate the groundwater flows at the landfill site.

A part of this study was to test PCA as a tool to trace groundwater from the ponds to a source. Another approach could have been to e.g. hydrological modelling, to examine groundwater flows. However, creating a model can be costly and time-consuming. A PFAS fingerprinting analysis with PCA is a time-effective and cheap approach, since free tools, such as R, with extended documentation are available online. It can present interesting correlations that was not sought for in the study, yet beneficial to create an overall picture. When performing similar studies, a PCA can be a good place to start an inquiry.

## References

- Abiriga, D., Vestgarden, L. S., and Klempe, H. (2020). "Groundwater contamination from a municipal landfill: Effect of age, landfill closure, and season on groundwater chemistry". In: *Science of the total environment* 737, p. 140307.
- Abunama, T., Moodley, T., Abualqumboz, M., Kumari, S., and Bux, F. (2021). "Variability of leachate quality and polluting potentials in light of leachate pollution index (LPI)—A global perspective". In: *Chemosphere* 282, p. 131119.
- Bonnet, B. F. (2018). "Mass Flow and Fate of Per- and Polyfluoroalkyl Substances in a Landfill in Uppsala, Sweden." Accessed 2022-02-23. Master Thesis, 30 hp. Swedish University of Agriculture. DOI: [https://stud.epsilon.slu.se/13052/1/bonnet\\_b\\_180109.pdf](https://stud.epsilon.slu.se/13052/1/bonnet_b_180109.pdf).
- Buck, R. C., Franklin, J., Berger, U., Conder, J. M., Cousins, I. T., De Voogt, P., Jensen, A. A., Kannan, K., Mabury, S. A., and Leeuwen, S. P. J. van (2011). "Perfluoroalkyl and polyfluoroalkyl substances in the environment: terminology, classification, and origins". In: *Integrated environmental assessment and management* 7.4, pp. 513–541.
- Cerne, O., Allard, A. S., Ek, M., Junestedt, C., and Svenson, A. (2007). *Utvärdering av behandlingsmetoder för lakvatten från deponier. Kemisk karaktärisering av lakvatten före och efter olika behandlingssteg på ett antal svenska deponier*. Accessed 2022-02-23. URL: <https://www.ivl.se/download/1834244ba71728fcb3f3f749/1591704448541/B1748.pdf>.
- Cheremisinoff, N. P. (2016). *Perfluorinated chemicals (PFCs): contaminants of concern*. John Wiley & Sons.
- Cimbritz, M. and Jönsson, K. (2017). *Partiklar i lakvatten från deponier och förorenade vatten från avfallsupplag - betydelse och avskiljning*. Accessed 2022-02-23. URL: [https://www.avfallsverige.se/aktuellt/nyhetsarkiv/artikel/partiklar-i-lakvatten-fran-deponier-och-foro-renade-vatten-fran-avfallsupplag-betydelse-och-avskilj/index.php?eID=tx\\_securedownloads&p=42&u=0&g=0&t=1645721180&hash=6cc067a75d461048dc21312355da1757a01fa476&file=/fileadmin/user\\_upload/Rapporter/2017/2017-07.pdf](https://www.avfallsverige.se/aktuellt/nyhetsarkiv/artikel/partiklar-i-lakvatten-fran-deponier-och-foro-renade-vatten-fran-avfallsupplag-betydelse-och-avskilj/index.php?eID=tx_securedownloads&p=42&u=0&g=0&t=1645721180&hash=6cc067a75d461048dc21312355da1757a01fa476&file=/fileadmin/user_upload/Rapporter/2017/2017-07.pdf).
- Dray, S. and Josse, J. (2015). "Principal component analysis with missing values: a comparative survey of methods". In: *Plant Ecology* 216.5, pp. 657–667. ISSN: 13850237, 15735052.

- ECHA (n.d.). *Perfluoroalkyl chemicals (PFAS)*. Accessed 2022-02-16. European Chemicals Agency. URL: <https://echa.europa.eu/hot-topics/perfluoroalkyl-chemicals-pfas>.
- Eriksson, J., Dahlin, S., Nilsson, I., and Simonsson, M. (2019). *Marklära (Swedish)*. Studentlitteratur AB, Lund. ISBN: 978-91-44-06920-3.
- Fuertes, I., Gómez-Lavín, S., Elizalde, M. P., and Urtiaga, A. (2017). “Perfluorinated alkyl substances (PFASs) in northern Spain municipal solid waste landfill leachates”. In: *Chemosphere* 168, pp. 399–407. DOI: <http://dx.doi.org/10.1016/j.chemosphere.2016.10.072>.
- Gleisner, M., Riise, J., Nilsson, M., Häggrot, J., and Pettersson, M. (2019). “Vägledning om att riskbedöma och åtgärda PFAS-föreningar inom förorenade områden”. In: *Naturvårdsverket. Report 6871*.
- Gobelius, L., Hedlund, J., Dürig, W., Tröger, R., Lilja, K., Wiberg, K., and Ahrens, L. (2018). “Per- and polyfluoroalkyl substances in Swedish groundwater and surface water: implications for environmental quality standards and drinking water guidelines”. In: *Environmental science & technology* 52.7, pp. 4340–4349. DOI: <https://doi.org/10.1021/acs.est.7b05718>.
- Golder (2004). *Tolkning av hydrogeologiska förhållanden vid Hovgården avfallsanläggning, Uppsala*. URL: <https://www.uppsalavatten.se/globalassets/dokument/om-oss/rapporter-och-exjobb/miljorapporter/miljorapport-2020-hovgarden.pdf>.
- Grandin, U. (2012). *Dataanalys och hypotesprövning för statistikanvändare. (Swedish)*.
- Gu, H., Chi, B., Li, H., Jiang, J., Qin, W., and Wang, H. (2015). “Assessment of groundwater quality and identification of contaminant sources of Liujiang basin in Qinhuangdao, North China”. In: *Environmental Earth Sciences* 73.10, pp. 6477–6493.
- Hamid, H., Li, L. Y., and Grace, J. R. (2018). “Review of the fate and transformation of per- and polyfluoroalkyl substances (PFASs) in landfills”. In: *Environmental Pollution* 235, pp. 74–84.
- Hansson, K., Palm Cousins, A., Norström, K., Graae, L., and Stenmarck, Å. (2016). *Sammanställning av befintlig kunskap om föroreningskällor till PFAS-ämnen i svensk miljö*. URL: <https://www.ivl.se/download/18.34244ba71728fcb3f3f9ef/1591705616515/C182.pdf>.
- Hartmann, K., Krois, J., and Waske, B. (2018). *E-Learning Project SOGA: Statistics and Geospatial Data Analysis (Interpretation and visualization)*. Accessed 2023-01-09. Freie Universitaet Berlin. URL: <https://www.geo.fu->

berlin.de/en/v/soga/Geodata-analysis/Principal-Component-Analysis/principal-components-basics/Interpretation-and-visualization/index.html.

- Helena, B., Pardo, R., Vega, M., Barrado, E., Fernandez, J. M., and Fernandez, L. (2000). “Temporal evolution of groundwater composition in an alluvial aquifer (Pisuerga River, Spain) by principal component analysis”. In: *Water research* 34.3, pp. 807–816.
- Helsel, D. R., Hirsch, R. M., Ryberg, K. R., Archfield, S. A., and Gilroy, E. J. (2020). *Statistical methods in water resources: U.S. Geological Survey Techniques and Methods, book 4, chapter A3, 458 p.* Supersedes USGS Techniques of Water-Resources Investigations, book 4, chapter A3, version 1.1. DOI: <https://doi.org/10.3133/tm4A3>.
- Huset, C. A., Barlaz, M. A., Barofsky, D. F., and Field, J. A. (2011). “Quantitative determination of fluorochemicals in municipal landfill leachates”. In: *Chemosphere* 82.10, pp. 1380–1386. DOI: 10.1016/j.chemosphere.2010.11.072.
- Jolliffe, I. T. (1986). *Principal Component Analysis*. Springer Series in Statistics. Springer-Verlag New York Inc. ISBN: 0-387-96269-7.
- Jolliffe, I. T. and Cadima, J. (2016). “Principal component analysis: a review and recent developments”. In: *Phil. Trans. R. Soc. A* 374:20150202.0000, p. 0000. DOI: <https://doi.org/10.1098/rsta.2015.0202>.
- KEMI (2022). *Per- and polyfluoroalkyl substances (PFAS)*. Accessed 2022-10-06. Swedish Chemical Agency. URL: <https://www.kemi.se/en/chemical-substances-and-materials/highly-fluorinated-substances>.
- Kjeldsen, P., Barlaz, M. A., Rooker, A. P., Baun, A., Ledin, A., and Christensen, T. H. (2002). “Present and long-term composition of MSW landfill leachate: a review”. In: *Critical reviews in environmental science and technology* 32.4, pp. 297–336. DOI: <https://doi.org/10.1080/10643380290813462>.
- Lenka, S. P., Kah, M., and Padhye, L. P. (2021). “A review of the occurrence, transformation, and removal of poly-and perfluoroalkyl substances (PFAS) in wastewater treatment plants”. In: *Water research* 199, p. 117187.
- Miljösamverkan Sverige (2022). *PFAS vid deponier*. URL: <https://www.miljosamverkansverige.se/wp-content/uploads/2022-01-27-Rapport-PFAS-vid-deponier.pdf>.

Naturvårdsverket (n.d.). *Högfluorerade ämnen i miljön, PFAS*. Accessed 2022-10-04. URL: <https://www.naturvardsverket.se/amnesomraden/miljoforeningar/organiska-miljogifter/hogfluorerade-amnen-i-miljon-pfas/>.

Olsen, R. W., Chappell, R. L., and Loftis, J. C. (2012). "Water quality sample collection, data treatment and results presentation for principal components analysis – literature review and Illinois River watershed case study". In: *Water Research* 46, p. 9. DOI: <https://doi.org/10.1016/j.watres.2012.03.028>.

Öman, C. B. and Junestedt, C. (2008). "Chemical characterization of landfill leachates—400 parameters and compounds". In: *Waste management* 28.10, pp. 1876–1891. DOI: <https://doi.org/10.1016/j.wasman.2007.06.018>.

Östman, M. (2008). "Ageing landfills - Development and Processes". PhD thesis. Swedish University of Agricultural Sciences.

Rhoads, K. R., Janssen, E. M.-L., Luthy, R. G., and Criddle, C. S. (2008). "Aerobic biotransformation and fate of N-ethyl perfluorooctane sulfonamidoethanol (N-EtFOSE) in activated sludge". In: *Environmental science & technology* 42.8, pp. 2873–2878.

Strawn, D. G. (2021). "Sorption Mechanisms of Chemicals in Soils". In: *Soil Systems* 5.1. ISSN: 2571-8789. DOI: 10.3390/soilsystems5010013. URL: <https://www.mdpi.com/2571-8789/5/1/13>.

Swedish Chemicals Agency (2020). *Gränsvärden och riktvärden för PFAS*. Accessed 2023-01-09. URL: <https://www.kemi.se/download/18.7729c777174435792104298/1599138086747/gransvarden-och-riktvarden-for-pfas.pdf>.

Swedish Food Agency (2022). *PFAS in drinking water and self-caught fish - risk management*. Accessed 2023-01-09. URL: <https://www.livsmedelsverket.se/en/business-legislation-and-control/drinking-water-production-and-control/t>.

Uppsala Vatten (2020). *MILJÖRAPPORT 2020 Hovgårdens avfallsanläggning*. URL: <https://www.uppsalavatten.se/download/18.6001eb69180b1f4d4304f3e1652254994098/Milj%5C%C3%5C%B6rapport%5C%202020%5C%20Hovg%5C%C3%5C%A5rden.pdf>.

Uppsala Vatten (2021). *Hovgårdens avfallsanläggning*. Accessed 2022-03-16. URL: <https://www.uppsalavatten.se/globalassets/dokument/>

hushall/blanketter-och-trycksaker/anlaggningspresentation-hovgarden-2021.pdf.

Uppsala Vatten och Avfall AB (n.d.). *Deponering*. Accessed 2022-02-21. URL: <https://www.uppsalavatten.se/foretag/avfall-och-atervinning/hovgardens-avfallsanlaggning/>.

USEPA (2022). *Our Current Understanding of the Human Health and Environmental Risks of PFAS*. Accessed 2022-10-04. US Environmental Protection Agency. URL: <https://www.epa.gov/pfas/our-current-understanding-human-health-and-environmental-risks-pfas>.

Wold, S., Esbensen, K., and Geladi, P. (1987). "Principal component analysis". In: *Chemometrics and intelligent laboratory systems 2.1-3*, pp. 37–52.

Yaqoob, M. M., Berta, C., Szabó, L. J., Dévai, G., Szabó, S., Nagy, S. A., Bácsi, I., Simon, A., Nagy, J., Somlyai, I., et al. (2021). "Changes in Algal Plankton Composition and Physico-Chemical Variables in a Shallow Oxbow Lake". In: *Water* 13.17, p. 2339.

## Appendix

### A Mass Balance

#### A.1 Sludge Pumping

$$t_{pumping} = 2 \text{ min}$$

$$t_{rest} = 60 \text{ min}$$

$$t_{tot} = 62 \text{ min}$$

$$Q_{pumping} = 5 \text{ L/s}$$

$$T = t_{tot}/t_{day} = (24 * 60) \text{ min/day} / 62 \text{ min} = 23.2258065 \text{ cycles/day}$$

$$V_{cycle} = Q * t_{pumping} = 5 \text{ L/s} * (2 * 60) \text{ s} = 600 \text{ L/cycle}$$

$$V_{day} = V_{cycle} * T = 600 \text{ L/cycle} * 23.2258065 \text{ cycles} = 13935.48387 \text{ L} = 13.935 \text{ m}^3/\text{day}$$

### B Charge Balance

Table 6: The charge balance for groundwater and pond data.

Sample	Date	Missing data	Net charge [mmol/l]
P1	2022-02-09	NO <sub>3</sub> <sup>-</sup> , Cl <sup>-</sup> , SO <sub>4</sub> <sup>2-</sup>	13
P2	2022-02-09	NO <sub>3</sub> <sup>-</sup> , Cl <sup>-</sup> , SO <sub>4</sub> <sup>2-</sup>	15
P3 IN	2022-02-09	NO <sub>3</sub> <sup>-</sup> , Cl <sup>-</sup> , SO <sub>4</sub> <sup>2-</sup>	28
P3 UT	2022-02-09	NO <sub>3</sub> <sup>-</sup> , Cl <sup>-</sup> , SO <sub>4</sub> <sup>2-</sup>	5.6
P6	2022-02-09	NO <sub>3</sub> <sup>-</sup> , Cl <sup>-</sup> , SO <sub>4</sub> <sup>2-</sup>	14
P8	2022-02-09	NO <sub>3</sub> <sup>-</sup> , Cl <sup>-</sup> , SO <sub>4</sub> <sup>2-</sup>	24
P24	2022-02-09	NO <sub>3</sub> <sup>-</sup> , Cl <sup>-</sup> , SO <sub>4</sub> <sup>2-</sup>	0.96
18G02	2022-02-09	NO <sub>3</sub> <sup>-</sup> , Cl <sup>-</sup> , SO <sub>4</sub> <sup>2-</sup>	0.46
18G09	2022-02-09	NO <sub>3</sub> <sup>-</sup> , Cl <sup>-</sup> , SO <sub>4</sub> <sup>2-</sup>	34
18G10	2022-02-09	NO <sub>3</sub> <sup>-</sup> , Cl <sup>-</sup> , SO <sub>4</sub> <sup>2-</sup>	10
H1C	2022-02-09	NO <sub>3</sub> <sup>-</sup> , Cl <sup>-</sup> , SO <sub>4</sub> <sup>2-</sup>	2.9
18G12	2022-02-09	NO <sub>3</sub> <sup>-</sup> , Cl <sup>-</sup> , SO <sub>4</sub> <sup>2-</sup>	10
PS mean	2022-02-23		0.16
PN mean	2022-02-23		0.0011

## C Mass Balance

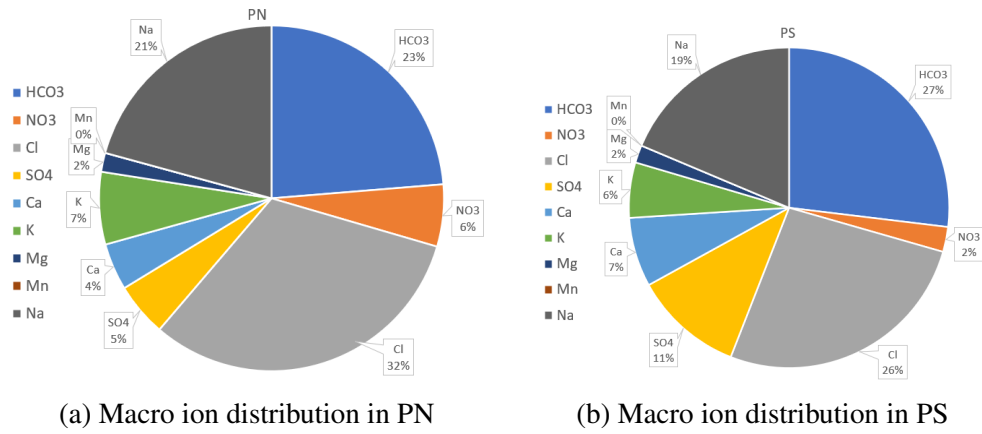


Figure 34: Macro ion distribution in the polishing ponds in May 10th, 2022.

## D PFAS

### D.1 PFAS abbreviations

Table 7: PFAS abbreviations

	Full name
PFBA	Perfluorobutanoic acid
PFPeA	Perfluoropentanoic acid
PFHxA	Perfluorohexanoic acid
PFHpA	Perfluoroheptanoic acid
PFOA	Perfluorooctanoic acid
PFNA	Perfluorononanoic acid
PFDA	Perfluorodecanoic acid
PFUnDA	Perfluoroundecanoic acid
PFDoDA	Perfluorododecanoic acid
PFTriDA	Perfluorotridecanoic acid
PFTeDA	Perfluorotetradecanoic acid
PFBS	Perfluorobutanesulfonic acid
PFPeS	Perfluoropentanesulfonic acid
PFHxS	Perfluorohexanesulfonic acid
PFHpS	Perfluoroheptanesulfonic acid
PFOS	Perfluorooctanesulfonic acid
6:2 FTSA	6:2 Fluorotelomer sulfonic acid
PFNS	Perfluorononanesulfonic acid
PFDS	Perfluorodecanesulfonic acid
PFDoDS	Perfluorododecanesulfonic acid
4:2 FTS	4:2 Fluorotelomer sulfonic acid
8:2 FTS	8:2 Fluorotelomer sulfonic acid
FOSA	Perfluorooctanesulfonamide
MeFOSA	Methylperfluorooctanesulfonamide
EtFOSA	Ethylperfluorooctanesulfonamid
MeFOSE	Methylperfluorooctanesulfonamidoethanol
EtFOSE	Ethylperfluorooctanesulfonamidoethanol
FOSAA	Perfluorooctanesulfonamidoacetic acid
MeFOSAA	Methylperfluorooctanesulfonamidoacetic acid
EtFOSAA	Ethylperfluorooctanesulfonamidoacetic acid
HPFHpA	7H-Dodecanfluorheptane acid
PF37DMOA	Perfluoro-3,7-dimethyloctanoic acid
PFAS $\Sigma$ 11	Sum of the following PFASs: PFBA, PFPeA, PFHxA, PFHpA, PFOA, PFNA, PFDA, PFBS, PFHxS, PFOS och 6:2 FTS

## D.2 PFAS concentration - all samples

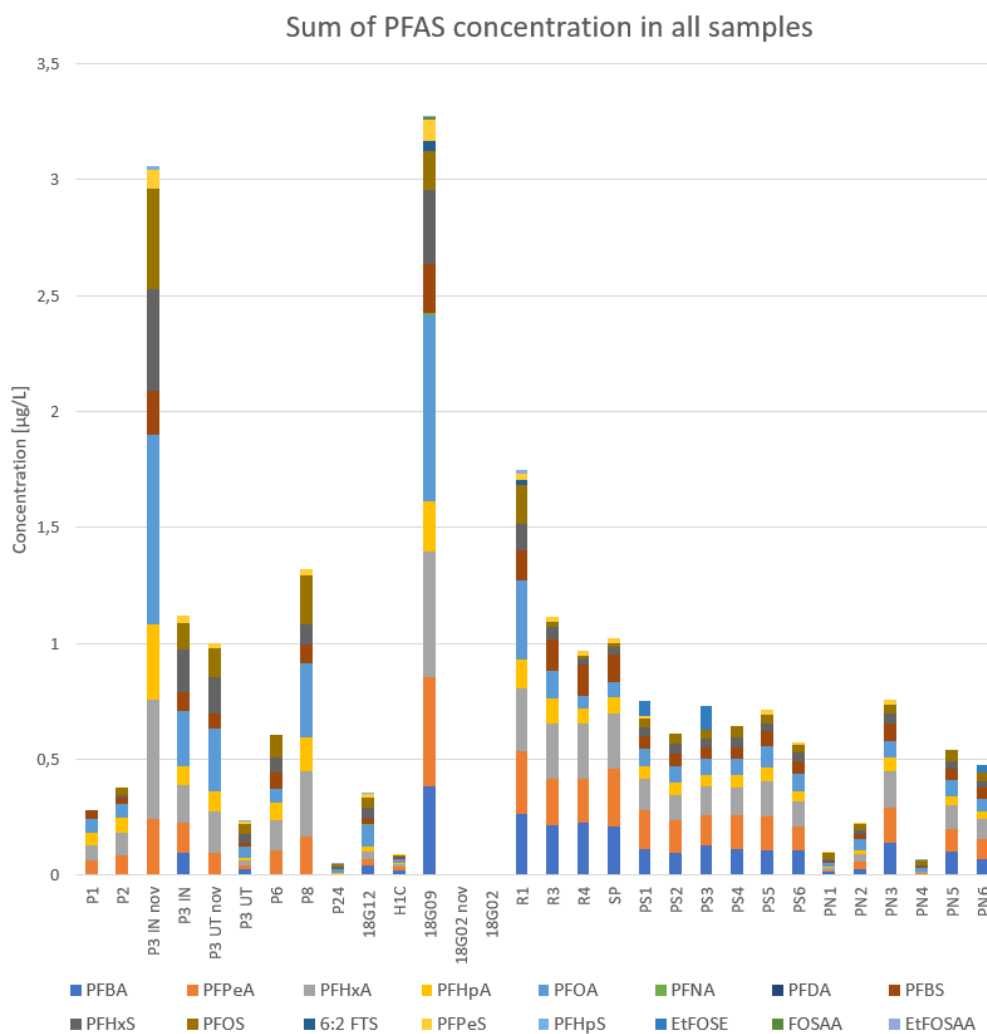


Figure 35: Concentration of PFAS in Hovgården. For P3 IN, P3 UT and 18G02, samples were taken both in March 2022 and November 2021.

### D.3 PFAS composition - all samples

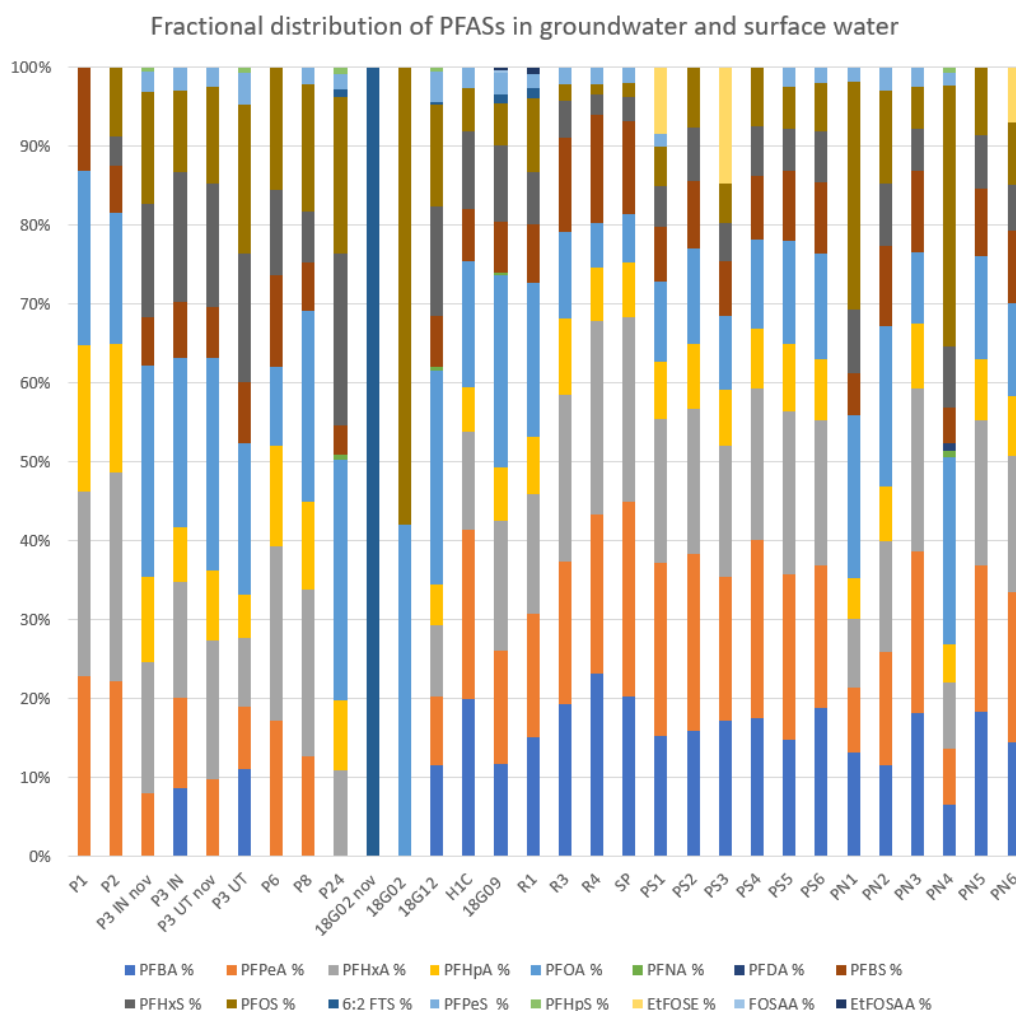


Figure 36: PFAS composition profile (fingerprint) of PFAS in Hovgården. For P3 IN, P3 UT and 18G02, samples were taken both in March 2022 and November 2021.

## E Correlation analysis for ions

### E.1 Correlation table for ions in the polishing ponds

	val	Temp	Cond	Al.µg.l	As.µg.l	Ba.µg.l	Ca.mg.l	Cd.µg.l	Co.µg.l	Cr.µg.l	Cu.µg.l	Fe.mg.l	K.mg.l	Mg.mg.l	Mn.µg.l	Mo.µg.l	Na.mg.l	Ni.µg.l	P.µg.l	Pb.µg.l	S.mg.l	Sb.µg.l	Si.mg.l	Sr.µg.l	V.µg.l	Zn.µg.l
Temp	r-value	1	0.00302	-0.0472	-0.283	0.183	-0.242	-0.509	-0.00414	0.331	-0.0861	-0.0682	0.258	0.235	-0.360	0.283	-0.0457	-0.452	0.414	-0.297	-0.0346	-0.720	-0.130	-0.416	-0.279	
	p-value	NA	0.985	0.766	0.0693	0.246	0.122	0.000573	0.979	0.0323	0.588	0.668	0.0989	0.134	1.89E-05	0.0191	0.0692	0.774	0.00268	0.00639	0.0565	0.828	7.51E-08	0.410	0.00613	0.0736
Cond	r-value		1	0.0103	-0.0823	0.436	0.0376	-0.119	0.570	0.310	0.234	0.0210	0.451	0.373	0.0976	-0.0162	0.419	0.335	-0.133	-0.00126	-0.113	-0.113	0.246	0.231	-0.209	0.0949
	p-value		NA	0.948	0.605	0.00387	0.813	0.455	7.99E-05	0.0459	0.136	0.895	0.00274	0.0150	0.539	0.919	0.00570	0.0301	0.400	0.994	0.478	0.477	0.116	0.142	0.185	0.550
Al.µg.l	r-value			1	0.272	0.259	-0.210	-0.359	0.492	0.0819	0.193	-0.0340	0.105	0.00766	-0.161	0.103	0.0819	0.491	0.175	-0.115	-0.295	0.338	0.123	-0.0792	0.225	0.243
	p-value			NA	0.161	0.0237	0.492	0.0105	1.62E-05	0.532	0.392	0.597	0.0378	0.182	0.144	0.359	0.0745	4.64E-05	0.268	0.275	0.0653	0.393	0.438	0.618	0.166	0.290
As.µg.l	r-value				1	-0.231	-0.467	-0.296	0.153	-0.0386	0.806	0.150	-0.357	-0.461	-0.0536	-0.222	-0.424	-0.00655	-0.0115	-0.204	-0.604	0.727	0.274	-0.474	0.901	0.897
	p-value				NA	0.162	0.00139	0.0648	0.410	0.801	2.55E-11	0.392	0.0302	0.00323	0.766	0.160	0.00821	0.966	0.942	0.206	1.34E-05	1.01E-07	0.0789	0.00151	4.44E-15	4.44E-16
Ba.µg.l	r-value					1	0.584	-0.00578	0.846	0.584	-0.0211	-0.0687	0.910	0.887	0.0402	0.581	0.914	0.900	0.0201	0.0106	0.329	-0.0864	0.462	0.805	-0.206	-0.105
	p-value					NA	5.98E-05	0.379	6.57E-14	4.53E-06	0.636	0.401	0	0	0.550	3.13E-05	0	0	0.899	0.501	0.0324	0.246	0.00209	1.33E-10	0.0885	0.262
Ca.mg.l	r-value						1	0.707	0.247	0.133	-0.369	-0.199	0.584	0.714	0.352	0.885	0.635	0.535	0.190	-0.135	0.931	-0.425	0.582	0.931	-0.233	-0.347
	p-value						NA	1.32E-06	0.0552	0.427	0.0123	0.135	7.27E-05	1.76E-07	0.0370	4.44E-16	7.64E-06	0.000160	0.227	0.328	0	0.00561	5.34E-05	0	0.142	0.0181
Cd.µg.l	r-value							1	-0.211	-0.245	-0.329	-0.162	-0.0120	0.140	0.489	0.699	0.0403	-0.00425	0.344	-0.251	0.786	-0.411	0.427	0.495	-0.0169	-0.242
	p-value							NA	0.0517	0.0466	0.0671	0.402	0.324	0.995	0.000160	3.40E-06	0.539	0.416	0.0257	0.290	1.26E-08	0.0647	0.00482	0.000854	0.837	0.243
Co.µg.l	r-value								1	0.521	0.361	0.0534	0.687	0.590	0.148	0.365	0.655	0.873	0.107	-0.0492	-0.0268	0.204	0.550	0.507	0.117	0.306
	p-value								NA	0.000391	0.0732	0.806	1.16E-09	3.25E-07	0.953	0.00782	9.85E-09	0	0.501	0.357	0.887	0.755	0.000163	0.000620	0.649	0.186
Cr.µg.l	r-value									1	0.112	0.00957	0.658	0.586	-0.102	0.135	0.615	0.468	-0.129	0.330	-0.0854	0.324	0.167	0.358	-0.0240	-0.0113
	p-value									NA	0.662	0.752	3.24E-06	3.19E-05	0.239	0.264	1.08E-05	0.000735	0.416	0.190	0.747	0.148	0.291	0.0200	0.424	0.652
Cu.µg.l	r-value										1	0.142	-0.129	-0.234	-0.0434	-0.188	-0.196	0.123	-0.121	0.0288	-0.542	0.685	0.238	-0.312	0.668	0.955
	p-value										NA	0.382	0.259	0.0814	0.967	0.209	0.132	0.695	0.446	0.683	9.58E-05	3.20E-07	0.129	0.0440	5.77E-07	0
Fe.mg.l	r-value											1	-0.228	-0.250	0.436	-0.218	-0.228	0.00862	0.255	0.515	-0.190	0.0746	-0.00151	-0.147	0.162	0.214
	p-value											NA	0.0991	0.0745	0.00273	0.0829	0.0917	0.524	0.104	0.000440	0.236	0.826	0.992	0.353	0.267	0.161
K.mg.l	r-value												1	0.980	-0.0777	0.495	0.993	0.780	-0.0876	0.117	0.332	-0.199	0.370	0.785	-0.350	-0.265
	p-value												NA	0	0.181	0.000760	0	4.47E-12	0.581	0.870	0.0505	0.0326	0.0160	7.44E-10	0.0220	0.0398
Mg.mg.l	r-value													1	-0.0295	0.590	0.991	0.746	-0.0699	0.107	0.497	-0.304	0.371	0.864	-0.402	-0.359
	p-value													NA	0.345	3.06E-05	0	1.11E-10	0.660	0.944	0.00170	0.00812	0.0155	1.66E-13	0.00724	0.00799
Mn.µg.l	r-value														1	0.338	-0.0585	0.142	0.492	0.0249	0.402	-0.198	0.530	0.314	0.119	0.0853
	p-value														NA	0.0558	0.245	0.970	0.000936	0.546	0.0121	0.519	0.000311	0.0425	0.307	0.393
Mo.µg.l	r-value															1	0.529	0.627	0.263	-0.248	0.772	-0.142	0.661	0.832	0.00512	-0.127
	p-value															NA	0.000218	4.88E-06	0.0925	0.0788	1.63E-09	0.400	1.93E-06	9.15E-12	0.928	0.361
Na.mg.l	r-value																1	0.772	-0.0808	0.116	0.401	-0.269	0.340	0.817	-0.398	-0.326
	p-value																NA	7.61E-12	0.611	0.938	0.0138	0.0150	0.0276	4.22E-11	0.00798	0.0147
Ni.µg.l	r-value																	1	0.144	0.0145	0.281	0.0666	0.609	0.719	0.0601	0.108
	p-value																	NA	0.363	0.546	0.0950	0.787	1.91E-05	8.08E-08	0.986	0.876
P.µg.l	r-value																		1	-0.0650	0.245	-0.0989	0.351	0.149	0.139	0.0237
	p-value																		NA	0.683	0.118	0.533	0.0225	0.347	0.381	0.882
Pb.µg.l	r-value																			1	-0.148	-0.0155	-0.350	-0.0653	-0.180	-0.0790
	p-value																			NA	0.287	0.690	0.0231	0.681	0.395	0.844
S.mg.l	r-value																				1	-0.548	0.417	0.798	-0.335	-0.490
	p-value																				NA	0.000315	0.00599	2.51E-10	0.0179	0.000513
Sb.µg.l	r-value																					1	0.0826	-0.364	0.629	0.715
	p-value																					NA	0.603	0.0178	2.89E-05	5.75E-08
Si.mg.L	r-value																						1	0.604	0.415	0.340
	p-value																						NA	2.32E-05	0.00629	0.0278
Sr.µg.l	r-value																							1	-0.288	-0.337
	p-value																							NA	0.0644	0.0289
V.µg.l	r-value																								1	0.789
	p-value																								NA	1.20E-10
Zn.µg.l	r-value																									1
	p-value																									NA

Table 37: Pearson correlation analysis of polishing pond ion data.

## **E.2 Correlation table for ions in groundwater**

		Alk	Ammonium	Tot_N	Cl	SO4	Al	As	Ba	Ca	Cd	Co	Cr	Cu	Fe	K	Mg	Mn	Mo	Na	Ni	P	Pb	S	Sb	Si	Sr	V	Zn	
Alk	r-value	1	0.709	0.259	0.722	0.369	-0.225	0.483	0.434	0.330	0.0786	0.676	0.242	0.175	0.106	0.790	0.660	0.734	0.366	0.843	0.117	-0.118	0.0458	0.344	0.288	0.345	0.564	0.365	-0.202	
	p-value		2.15E-07	0.0344	4.57E-07	0.0282	0.263	0.000118	0.00168	0.0389	0.798	4.72E-08	0.0159	0.772	0.727	8.75E-14	1.94E-07	1.61E-09	0.0005	2.22E-16	0.371	0.335	0.762	0.0413	0.231	0.0103	2.84E-05	0.0541	0.130	
Ammonium	r-value		1	0.541	0.482	0.0405	-0.0885	0.322	0.391	0.0684	0.0726	0.625	0.402	0.296	-0.0734	0.565	0.300	0.820	0.147	0.565	0.167	-0.0761	0.000444	0.0306	0.297	0.429	0.257	0.130	-0.066	
	p-value			0.00140	0.00371	0.799	0.501	0.220	0.0955	0.944	0.973	0.00320	0.234	0.465	0.554	0.0131	0.388	0.000213	0.439	0.0297	0.356	0.517	0.777	0.721	0.00247	0.124	0.389	0.940	0.695	
Tot_N	r-value			1	0.178	0.248	-0.152	0.10737	0.319	0.353	0.282	0.511	0.142	0.703	-0.181	0.253	0.176	0.389	0.00906	0.206	0.836	0.593	0.00546	0.257	0.586	0.414	0.166	-0.0808	0.780	
	p-value				0.347	0.186	0.407	0.328	0.0374	0.0430	0.141	0.000102	0.132	3.21E-06	0.313	0.0317	0.182	0.0114	0.296	0.0711	2.65E-12	1.91E-05	0.969	0.124	3.51E-05	0.00369	0.304	0.713	3.66E-07	
Cl	r-value				1	0.430	-0.06407	0.583	0.778	0.603	0.602	0.671	0.317	0.494	0.0281	0.965	0.875	0.749	0.305	0.934	0.290	-0.072	0.541	0.437	0.523	0.197	0.930	0.319	-0.207	
	p-value					0.0087	0.745	0.000281	1.11E-08	3.33E-05	3.40E-05	5.05E-06	0.0805	0.00109	0.948	0	2.56E-12	1.69E-07	0.150	0	0.0666	0.697	0.000581	0.00806	0.00857	0.268	0	0.123	0.228	
SO4	r-value					1	-0.00835	0.227	0.468	0.769	0.108	0.299	0.175	0.255	0.411	0.420	0.758	0.243	0.0349	0.500	0.439	0.390	0.185	0.992	0.239	0.435	0.520	0.358	0.270	
	p-value						0.859	0.187	0.00347	3.41E-08	0.508	0.0652	0.227	0.161	0.0187	0.0121	5.99E-08	0.111	0.763	0.00202	0.00949	0.0203	0.246	0	0.503	0.00401	0.00094	0.0847	0.143	
Al	r-value						1	-0.147	0.127	-0.0248	0.0361	-0.0223	0.839	0.0595	0.182	-0.118	-0.04786	-0.0936	-0.232	-0.133	-0.0541	0.0155	0.434	0.0144	-0.05078	0.168	-0.0595	0.434	-0.100	
	p-value							0.535	0.343	0.760	0.867	0.899	1.60E-12	0.516	0.0296	0.523	0.980	0.584	0.111	0.578	0.725	0.666	0.000268	0.559	0.598	0.117	0.938	0.00017	0.581	
As	r-value							1	0.476	0.366	0.360	0.357	0.128	0.396	-0.0854	0.633	0.572	0.445	0.160	0.622	0.168	-0.14592	-0.0670	0.265	0.280	0.0529	0.608	0.00810	-0.141	
	p-value								0.00127	0.0138	0.0272	0.00244	0.111	0.0291	0.825	3.15E-07	1.13E-05	0.0005	0.120	4.27E-07	0.240	0.497	0.936	0.0670	0.245	0.320	3.43E-06	0.436	0.412	
Ba	r-value								1	0.810	0.761	0.503	0.429	0.662	0.220	0.687	0.690	0.693	0.150	0.623	0.444	0.116	0.687	0.525	0.58	0.308	0.824	0.264	0.0223	
	p-value									3.25E-12	1.27E-08	0.000213	0.00301	5.96E-05	0.172	4.84E-07	7.81E-08	4.97E-07	0.396	3.24E-06	0.00543	0.532	8.04E-07	0.000144	0.00525	0.0400	2.04E-12	0.176	0.956	
Ca	r-value									1	0.644	0.375	0.161	0.627	0.209	0.52279	0.761	0.359	0.125	0.490	0.626	0.406	0.543	0.818	0.606	0.299	0.7672	0.222	0.312	
	p-value										3.49E-06	0.00785	0.152	2.51E-05	0.165	0.00087	3.18E-10	0.0274	0.934	0.0009	5.54E-05	0.00933	7.31E-05	6.64E-13	0.00982	0.0297	1.02E-10	0.143	0.104	
Cd	r-value										1	0.374	0.138	0.810	-0.241	0.487	0.449	0.373	0.120	0.338	0.558	0.166	0.727	0.182	0.759	-0.07094	0.724	-0.0922	0.189	
	p-value											0.0152	0.531	7.62E-10	0.134	0.00400	0.0034	0.0210	0.998	0.0483	0.00034	0.282	2.87E-07	0.294	1.43E-05	0.515	7.09E-08	0.532	0.257	
Co	r-value											1	0.374	0.584	-0.141	0.649	0.526	0.705	0.397	0.650	0.504	0.122	0.25	0.277	0.530	0.353	0.637	0.0671	0.141	
	p-value												0.00112	0.00013	0.640	2.17E-08	2.72E-05	2.67E-08	0.00536	2.86E-08	9.54E-05	0.240	0.0589	0.0494	0.00225	0.00370	9.96E-07	0.380	0.280	
Cr	r-value												1	0.265	0.264	0.313	0.273	0.409	-0.075	0.310	0.110	0.0176	0.433	0.190	0.180	0.435	0.233	0.581	-0.113	
	p-value													0.0961	0.00664	0.00670	0.0197	0.00228	0.853	0.00408	0.358	0.584	0.000342	0.0972	0.550	0.000285	0.0483	7.25E-07	0.575	
Cu	r-value													1	-0.274	0.466	0.419	0.420	0.0947	0.347	0.866	0.538	0.465	0.308	0.855	0.202	0.590	-0.0974	0.561	
	p-value														0.247	0.0252	0.0185	0.0717	0.653	0.102	3.95E-14	1.83E-06	0.000860	0.052	6.44E-08	0.215	0.00028	0.921	5.30E-07	
Fe	r-value														1	0.0266	0.140	0.133	-0.0617	0.117	-0.175	0.0190	0.0574	0.400	-0.312	0.365	0.0175	0.563	-0.153	
	p-value															0.937	0.531	0.421	0.449	0.599	0.293	0.54	0.176	0.0118	0.0489	0.00308	0.931	7.29E-06	0.425	
K	r-value															1	0.865	0.761	0.287	0.977	0.302	-0.0382	0.371	0.418	0.522	0.248	0.849	0.368	-0.160	
	p-value																1.16E-13	2.14E-10	0.00349	0	0.0374	0.729	0.0278	0.0128	0.0163	0.0468	2.08E-12	0.0428	0.318	
Mg	r-value																1	0.554	0.190	0.879	0.365	0.0732	0.404	0.764	0.474	0.279	0.876	0.384	-0.0524	
	p-value																	6.35E-05	0.214	2.22E-15	0.0181	0.703	0.00732	5.21E-10	0.0747	0.0265	0	0.0281	0.699	
Mn	r-value																	1	0.204	0.755	0.208	-0.136	0.280	0.244	0.399	0.408	0.590	0.186	-0.172	
	p-value																		0.0513	3.47E-10	0.210	0.305	0.111	0.144	0.0938	0.00203	2.85E-05	0.361	0.196	
Mo	r-value																		1	0.290	0.0517	-0.132	0.0673	0.0223	0.310	-0.1535	0.318	-0.0417	-0.111	
	p-value																			0.00717	0.673	0.361	0.810	0.687	0.134	0.5736	0.111	0.882	0.400	
Na	r-value																			1	0.229	-0.0683	0.272	0.485	0.400	0.272	0.807	0.420	-0.202	
	p-value																				0.111	0.620	0.0709	0.00179	0.105	0.0232	1.10E-11	0.0118	0.203	
Ni	r-value																				1	0.705	0.250	0.464	0.759	0.294	0.415	-0.0465	0.856	
	p-value																					1.09E-09	0.145	0.00356	4.92E-07	0.0292	0.0106	0.736	7.15E-14	
P	r-value																						1	0.09746	0.394	0.403	0.288	0.0385	0.103	0.730
	p-value																							0.369	0.00911	0.0398	0.0222	0.877	0.313	7.47E-12
		Alk	Ammonium	Tot_N	Cl	SO4	Al	As	Ba	Ca	Cd	Co	Cr	Cu	Fe	K	Mg	Mn	Mo	Na	Ni	P	Pb	S	Sb	Si	Sr	V	Zn	
Pb	r-value																							1	0.230	0.462	0.0314	0.574	0.248	-0.0756
	p-value																								0.0922	0.0257	0.511	4.10E-05	0.00706	0.